

Mean-field theories of the two-band model and the magnetism in high- T_c oxides

Andrzej M. Oleś* and Jan Zaanen

Max-Planck-Institut für Festkörperforschung, D-7000 Stuttgart 80, Federal Republic of Germany

(Received 24 October 1988)

The antiferromagnetic ground state of a two-band model Hamiltonian which describes $\text{Cu}(3d_{x^2-y^2})$ and $\text{O}(2p_{x(y)})$ orbitals within a CuO_2 plane, a common structural unit of high- T_c superconducting oxides (HTSO) is studied by using a Hartree-Fock approximation (HFA) and the Gutzwiller ansatz (GA). Using the GA, a weak-coupling effective Stoner theory is derived in the low hole density limit. Compared to HFA, the Stoner parameter is strongly reduced, showing that correlations tend to weaken the magnetic instability in this limit. In the localized limit both the HFA and the GA converge to the same solution, corresponding to a classical Heisenberg system with the correct superexchange. We point out that the local spin-density approximation has intrinsic difficulties for the present problem. For intermediate d -hole densities numerical results are obtained and the magnetism of the HTSO is discussed. We argue that, in spite of its qualitative success, the model cannot account at the same time for the known magnetic and electronic properties of the HTSO.

I. INTRODUCTION

Although there is yet no consensus concerning the mechanism of superconductivity in high- T_c superconducting oxides (HTSO), there are numerous indications that it may be of electronic nature. Such experimental results as high values of T_c accompanied by rather low values of the density of states at the Fermi level, or the absence of isotope effect in $\text{YBa}_2\text{Cu}_3\text{O}_{6+x}$, are not easy to explain by the conventional theory. Therefore, numerous nonphonon mechanisms of superconductivity have been proposed, as reviewed recently by Fulde,¹ Varma,² and Cyrot.³ It may be concluded from these reviews that the high values of T_c cannot be understood by electron-phonon interaction and the search for an electronic mechanism is necessary. It may be realized that it is not easy to discuss particular microscopic mechanisms of pairing without having a deeper understanding of the electronic properties of the normal phase of HTSO. Therefore, we believe that the latter issue should be the first goal on a way to the microscopic theory of superconductivity in this new class of materials.

It is remarkable that the systems $\text{La}_{2-x}\text{Sr}_x\text{CuO}_4$ and $\text{YBa}_2\text{Cu}_3\text{O}_{6+x}$, where $x > 0$, have rather similar phase diagrams.⁴⁻⁷ The antiferromagnetic (AF) order disappears quickly with doping (i.e., for $x > 0$) and both systems, $\text{La}_{2-x}\text{Sr}_x\text{CuO}_4$ and $\text{YBa}_2\text{Cu}_3\text{O}_{6+x}$, become superconducting at higher values of x .⁴⁻⁷ Magnetic order, most likely AF, has also been detected recently in $\text{Bi}_2\text{Sr}_2\text{CaCu}_2\text{O}_8$ below 250 K.⁸ The presence of antiferromagnetism in the vicinity of superconducting (SC) phase in the phase diagrams of HTSO suggests that AF correlations may play an important role in the actual mechanism of pairing. In fact, several mechanisms which originate from the AF interactions, such as resonating valence bonds⁹ (RVB), spin bags,¹⁰ pairing due to oxygen holes,¹¹ and others have been proposed so far.

The AF ground state of HTSO is of fundamental interest in itself. For $x=0$ both systems are found to be AF and have large magnetic moments which amount to

$\approx 0.4\mu_B$ in La_2CuO_4 ,⁵ and even up to $0.64\mu_B$ – $0.66\mu_B$ in $\text{YBa}_2\text{Cu}_3\text{O}_6$.^{6,7} There are indications that the AF and SC phases are separated by another phase which resembles a spin glass.¹² It is very spectacular that although a three-dimensional (3D) long-range order (LRO) collapses in $\text{La}_{2-x}\text{Sr}_x\text{CuO}_4$ above the critical doping $x_c \approx 0.03$, strong AF correlations exist within the CuO_2 planes both in the spin-glass and in the SC phase, with the correlation length being proportional to $x^{-1/2}$.¹³ It has been argued recently¹⁴ that the antiferromagnetism and its collapse may be quite well understood in terms of a localized model. The principal argument here is that a 2D Heisenberg model gives a magnetic moment between $0.36\mu_B$ (Ref. 14) and $0.38\mu_B$ (Ref. 15) which is thus considerably reduced from $1\mu_B$ due to quantum fluctuations and agrees qualitatively with what is observed in undoped HTSO. It has been also found that the spin-spin correlation function $S(q)$ of a 2D Heisenberg model reproduces quite well the experimental results for La_2CuO_4 .¹⁵ Furthermore, it has been suggested¹⁶ that the Kondo-like exchange interaction should give frustration of AF Cu–Cu bonds under doping since it competes with the superexchange interaction.

It is certainly true that HTSO are characterized by important electronic correlation effects. On the other hand, it is hard to believe that these effects lead to a *complete* localization of the $3d$ electrons. Apart from the magnetic data, all other information about the electronic structure seems to indicate that the HTSO are characterized by strong covalency and appreciable band-formation effects. This is suggested by local-density-approximation (LDA) calculations,^{17,18} also in conjunction with correlated models,¹⁹⁻²¹ and supported by photoemission data.²²⁻²⁵ Recently direct evidence for band formation has been supplied by angular resolved photoemission-^{26,27} and positron-annihilation measurements.²⁸

In this paper we will attempt to analyze the magnetic properties, starting out with what is known about the electronic structure. As a starting point we use the well-

known two-band Hamiltonian^{10,29} (see Sec. II) as a model for the electronic structure. The credit for this model comes from its success in describing the large energy scale data such as photoemission^{30,31} and, as in the case of Ce compounds, it seems reasonable to expect that it can also account for the low-energy magnetic properties in a semi-quantitative way. There is not much debate about the largeness of the on site d - d Coulomb energy (U) compared to the bandwidth (W). The basic problem is that the charge transfer energy D ,³⁰ describing the energy cost for p - d charge fluctuations, is probably rather small.²¹ This moves the system away from integral valency such that strong-coupling theory³² breaks down. The bands are expected to be moderately renormalized with the consequence that the magnetism is of a more collective (itinerant) kind. The new aspect compared with the one-band Hubbard model is that the strength of the correlations, and therefore the magnetism, is in first order dependent on the d -hole count¹⁹ and not on U , while the system is always at half filling. To our knowledge not much is known about this situation.

A first guess can be obtained from a simple Hartree-Fock approximation (HFA), as worked out in Sec. II. It has been known for a long time that the HFA produces the correct superexchange expression in the strong coupling (large D, U) limit,³³ although the quantum motion of the spins is lost because of the scalar nature of the HFA amplitudes. The success of HFA in this limit comes from the correct behavior with respect to the suppression of charge fluctuations. In the fully polarized (ferromagnetic or AF) case these are projected out automatically (see Sec. II). However, for low d -hole density and large U , HFA appears to be in error. As we will show, the *effective* Stoner parameter I_{eff} , i.e., the field which breaks the magnetic symmetry, goes there as $U\langle n_d \rangle$, where $\langle n_d \rangle$ stands for the average d -hole density. So for sufficiently large U this would always result in a strong-coupling situation for arbitrarily small D , which is obviously untrue. Correlation effects lead to an important renormalization of the Stoner parameter, as is well known for the elemental $3d$ metals. For instance, the U of Ni metal, as determined from photoemission experiments, is ≈ 3 eV,³⁴ while the Stoner parameter used to describe the magnetism is much smaller (≈ 0.7 eV).³⁵ A better approximate method is the mean-field approximation to the Gutzwiller ansatz (GA), which we discuss in Sec. III. Although in this approximation the quantum spin motion is neglected as well, the charge fluctuations are treated in a much better way. We will show that the GA becomes identical to the HFA in the strong-coupling regime, while it is much better behaved for small $\langle n_d \rangle$ where a weak-coupling Stoner theory is obtained for large values of U . In Sec. IV we evaluate HFA and GA in the intermediate-coupling regimes numerically, arriving at the conclusion that the HFA is in fact doing better here than expected beforehand. Finally, in Sec. V, we turn to the magnetism of HTSO and discuss the implications of our itinerant model. Our findings give a possible clue to the failure of local-spin-density-functional approximation (LSDA) to describe the intermediate coupling HTSO magnetism. Further, we demonstrate that the experimental data obtained for HTSO are, in a quantitative sense,

remarkably consistent with our model. Due to the approximations made, this should not be the case, pointing out some missing ingredient involved, and we speculate about possible ways out.

II. MODEL HAMILTONIAN AND HARTREE-FOCK APPROXIMATION

The results of the band-structure calculations of different compounds belonging to the class of HTSO are quite coherent.¹⁸ They predict that half-filled bands are present in the band structures of undoped systems: La_2CuO_4 ,¹⁷ $\text{YBa}_2\text{Cu}_3\text{O}_6$,³⁶ as well as in $\text{Bi}_2\text{Sr}_2\text{CaCu}_2\text{O}_8$,³⁷ and in $\text{Tl}_2\text{Ba}_2\text{CuO}_6$.³⁸ These bands have anti-bonding character and are built by $\text{Cu}(3d_{x^2-y^2})$ and $\text{O}(2p_{x(y)})$ orbitals of CuO_2 planes, a common structural unit of all HTSO. Their number is directly related to the number of CuO_2 planes in the unit cell of a considered superconductor. This suggests the following model Hamiltonian which describes holes in $\text{Cu}(3d_{x^2-y^2})$ and $\text{O}(2p_{x(y)})$ orbitals of the CuO_2 plane

$$H = \varepsilon_d \sum_{i,\sigma} d_{i\sigma}^\dagger d_{i\sigma} + \varepsilon_p \sum_{m,\sigma} a_{m\sigma}^\dagger a_{m\sigma} + U \sum_i d_{i\uparrow}^\dagger d_{i\downarrow}^\dagger d_{i\uparrow} d_{i\downarrow} + V \sum_{\langle i,m \rangle \sigma} (d_{i\sigma}^\dagger a_{m\sigma} + \text{H.c.}). \quad (2.1)$$

$d_{i\sigma}^\dagger (a_{m\sigma}^\dagger)$ stands for a creation operator of a hole in a $3d_{x^2-y^2}$ orbital at site i and in a $2p_{x(y)}$ orbital at site m , respectively. The summation in the last term, which describes hybridization between $3d$ and $2p$ orbitals, is restricted to nearest neighbors i and m . The Hamiltonian (2.1) describes the hole system in terms of three parameters: (i) hybridization energy V , (ii) charge transfer energy $D = \varepsilon_p - \varepsilon_d$, and (iii) Coulomb interaction at $d_{x^2-y^2}$ orbitals U . Depending on the values of these parameters, the system exhibits either localized or itinerant behavior.³²

The band-structure calculations performed by using LSDA give very useful information concerning the values of electronic parameters for HTSO. There is considerable evidence that $V \approx 1.5$ eV.²¹ The value of D was estimated to be relatively small, between 0–1 eV (Ref. 21) and ≈ 2 eV,^{38,39} which suggests an itinerant behavior.³² It is also evident that the value of U is large, of the order of 8 eV,²¹ but this value is known with less accuracy. In fact, different values of this parameter were reported by different groups: 8 eV, 10–12 eV, and 8–10 eV, by Zaanen *et al.*,²¹ Schluter, Hybertsen, and Christensen,³⁹ and Stechel and Jennison,⁴⁰ respectively. The two latter calculations were performed in such a way as to give a finite value of the on-oxygen Coulomb interactions between p holes (U_p) as well as of the intersite interaction between d and p holes (U_{dp}). If one does the HFA, however, all three sets appear to be consistent in predicting rather similar band structure following from the model Hamiltonian (1). The mapping of the band structure obtained from the parameters of Refs. 39 and 40, on the one which follows from (2.1) (under neglect of U_p and U_{dp}), gives a value of U between 5 and 7 eV. An addition-

al argument for the relative unimportance of U_p follows from the actual charge distribution of a single hole over the CuO_2 unit, giving a particularly low probability of a two-hole on-oxygen configuration for realistic model parameters.¹⁹ The parameter U_{dp} is important for the charge distribution but not for the magnetic order in which we are interested below.

In any case, the above shows that one is in the charge-transfer (CT) and *not* in the Mott-Hubbard (MH) regime of the phase diagram introduced for transition-metal oxides³⁰ and that the HTSO are mixed-valence materials.³² This point of view is also supported by the results of photoemission and core-emission experiments,²²⁻²⁵ which indicate that the values of V , D , and U are not very different from those of CuO .²¹ The charge transfer energy D was found to be either 0-1 eV (Ref. 23) or 2.75 eV,²⁵ depending on whether it was related to the lowest-energy excitation, or to the middle of the p band. The Coulomb element was estimated to be at least 4-5 eV (Ref. 22) or 6-7 eV.²³ In the analysis of the experimental data only the presence of Coulomb interaction on $3d_{x^2-y^2}$ was assumed, similarly as in our model Hamiltonian (2.1). Altogether, the results of LSDA calculations and the experimental data indicate that V and D are of the same order and that $U \gg D$. Motivated by that, we fix below the ratio $U/V=5$ for most of our numerical analysis

$$H_0 = \sum_{\mathbf{k}, \sigma} \begin{pmatrix} \varepsilon_{d,\text{HF}} & V_{\mathbf{k}} & v & 0 \\ V_{\mathbf{k}} & \varepsilon_p & 0 & 0 \\ v & 0 & \varepsilon_{d,\text{HF}} & V_{\mathbf{k}+\mathbf{Q}} \\ 0 & 0 & V_{\mathbf{k}+\mathbf{Q}} & \varepsilon_p \end{pmatrix} \begin{pmatrix} d_{\mathbf{k},\sigma} \\ a_{\mathbf{k},\sigma} \\ d_{\mathbf{k}+\mathbf{Q},\sigma} \\ a_{\mathbf{k}+\mathbf{Q},\sigma} \end{pmatrix}, \quad (2.4)$$

where

$$V_{\mathbf{k}} = V\gamma_{\mathbf{k}}, \quad (2.5)$$

$$\gamma_{\mathbf{k}} = 2(\cos^2 \frac{1}{2} k_m + \cos^2 \frac{1}{2} k_n)^{1/2}, \quad (2.6)$$

and $\mathbf{k} = (k_m, k_n)$. The resulting ground state is just a product of the occupied one-hole states with the energies lower than the (hole) Fermi energy E_F . In the nonmagnetic (NM) case (at $v=0$), the solution of Eq. (2.3) is straightforward. The quasiparticle states are obtained by diagonalizing the Hamiltonian (2.4) with a canonical transformation

$$\begin{pmatrix} \alpha_{\mathbf{k},\sigma} \\ \beta_{\mathbf{k},\sigma} \end{pmatrix} = \begin{pmatrix} \xi_{\mathbf{k}} & \zeta_{\mathbf{k}} \\ -\zeta_{\mathbf{k}} & \xi_{\mathbf{k}} \end{pmatrix} \begin{pmatrix} d_{\mathbf{k},\sigma} \\ a_{\mathbf{k},\sigma} \end{pmatrix}. \quad (2.7)$$

In this way one finds for the bonding and antibonding states

$$e_{\mathbf{k}}^{\pm} = \frac{1}{2} (\varepsilon_p + \varepsilon_{d,\text{HF}}) \pm \frac{1}{2} [(\varepsilon_p - \varepsilon_{d,\text{HF}})^2 + 4V_{\mathbf{k}}^2]^{1/2}. \quad (2.8)$$

This band structure has a perfect nesting property for the filling of $N=1$ hole per CuO_2 unit (half-filled bonding state) and is therefore unstable with respect to AF long-range order at finite values of U , with the local density of σ -spin holes within the $3d_{x^2-y^2}$ orbital of the form

$$n_{i\sigma} = \langle d_{i\sigma}^\dagger d_{i\sigma} \rangle = \frac{1}{2} \langle n_d \rangle \pm m \exp(i\mathbf{Q} \cdot \mathbf{R}_i), \quad (2.9)$$

in Sec. IV and vary D/V . We would like to emphasize that small D means that one-hole levels of energies ε_d and ε_p are close to each other. The electronic levels $\varepsilon_d^{\text{el}}$ and $\varepsilon_p^{\text{el}}$ on the contrary, differ by a large energy of the order of U since $\varepsilon_d^{\text{el}} = -\varepsilon_d - U$ and $\varepsilon_p^{\text{el}} = -\varepsilon_p$.

The AF phase is studied in the HFA by solving a Hamiltonian H_0 in place of H ,

$$H_0 = \sum_{i,\sigma} (\varepsilon_{d,\text{HF}} + v_{i\sigma}) d_{i\sigma}^\dagger d_{i\sigma} + \varepsilon_p \sum_{m,\sigma} a_{m\sigma}^\dagger a_{m\sigma} + V \sum_{(i,m)\sigma} (d_{i\sigma}^\dagger a_{m\sigma} + \text{H.c.}), \quad (2.2)$$

where $\varepsilon_{d,\text{HF}} = \varepsilon_d + \frac{1}{2} U \langle n_d \rangle$ is the d -hole energy in the HFA and $\langle n_d \rangle$ is the average hole density at d orbital. The interaction term proportional to U is replaced by an alternating field

$$v_{i\sigma} = \mp v \exp(i\mathbf{Q} \cdot \mathbf{R}_i). \quad (2.3)$$

The wave vector $\mathbf{Q} = (\pi/a, \pi/a)$ corresponds to the two-sublattice AF structure observed in HTSO; the signs correspond to $\sigma = \uparrow$ and \downarrow . This Hamiltonian may be easily diagonalized in \mathbf{k} space. In the geometry of CuO_2 plane, one obtains a nonbonding dispersionless band at energy ε_p , built of $2p$ orbitals. The remaining bonding and antibonding states follow from the diagonalization

where m is the magnetic moment. The average $\langle \dots \rangle$ is performed with respect to the ground state of H_0 . The total energy of the system,

$$E_0^{\text{HF}} = \langle H_0 \rangle + \langle H - H_0 \rangle, \quad (2.10)$$

may be then written as follows

$$E_0^{\text{HF}} = E_{\text{kin}}(0) + \Delta E_{\text{kin}}(m) + \frac{1}{4} U (\langle n_d \rangle^2 - m^2), \quad (2.11)$$

where E_{kin} and $\Delta E_{\text{kin}}(m)$ stand for the kinetic energy in the NM Hartree-Fock (HF) state and for the change of the kinetic energy due to AF order, respectively. The remaining part expresses the interaction energy. Its magnetic part is conventionally written as $-\frac{1}{4} I m^2$, where I is the Stoner parameter. It is evident that the latter is equal to U in our model and that $v = \frac{1}{2} Um$.

In general, the AF ground state has to be found numerically by minimizing the energy expression E_0^{HF} and determining thereby $\langle n_d \rangle$ and m in a self-consistent way. Before we present the results obtained from such a minimization procedure, let us consider the AF gap. The filling with one hole per CuO_2 unit results in an AF insulating state. The gap varies along the 2D Fermi surface and has a minimum at $\mathbf{Q} = (\pi/a, \pi/a)$, which is

$$\Delta = \frac{1}{2} Um + \frac{1}{2} \{ [(D_{\text{HF}} + \frac{1}{2} Um)^2 + 16V^2]^{1/2} - [(D_{\text{HF}} - \frac{1}{2} Um)^2 + 16V^2]^{1/2} \}, \quad (2.12)$$

where $D_{\text{HF}} = D - \frac{1}{2}U\langle n_d \rangle$ is the charge transfer energy for the renormalized one-particle d - and p -hole levels in the HFA. In the limit of small magnetization m (weakly magnetic system), Eq. (2.10) may be written in the form

$$\Delta(m \approx 0) = \frac{1}{2}Um \left[1 + \frac{D_{\text{HF}}}{(D_{\text{HF}} + 16V^2)^{1/2}} \right]. \quad (2.13)$$

Thus, our model Hamiltonian (1) reproduces the AF gap of the Hubbard model⁴¹ given by the product Um in the limit of $V, U \ll D_{\text{HF}}$, i.e., when the HF charge transfer energy D_{HF} is the largest energy in the problem. On the other hand, if $U < D$, the AF gap is substantially reduced, being only half of the value of the Hubbard model at $D_{\text{HF}} = 0$. This shows that the AF state is quite different, depending on the actual relations between the parameters of the Hamiltonian (2.1) and the gap is reduced by covalency.

In order to investigate further the analytic properties of the AF state in HFA, let us consider a simplified symmetry-broken solution which involves only the bonding hole subband $\varepsilon_{\mathbf{k}}^-$. In this case, the matrix of Eq. (2.4) reduces to

$$H_0^- = \sum_{\mathbf{k}, \sigma} (c_{\mathbf{k}, \sigma}^\dagger c_{\mathbf{k}+\mathbf{Q}, \sigma}^\dagger) \begin{pmatrix} \varepsilon_{\mathbf{k}}^- & \tilde{v}_{\mathbf{k}, \mathbf{k}+\mathbf{Q}} \\ \tilde{v}_{\mathbf{k}, \mathbf{k}+\mathbf{Q}} & \varepsilon_{\mathbf{k}+\mathbf{Q}}^- \end{pmatrix} \begin{pmatrix} c_{\mathbf{k}, \sigma} \\ c_{\mathbf{k}+\mathbf{Q}, \sigma} \end{pmatrix}, \quad (2.14)$$

where

$$\tilde{v}_{\mathbf{k}, \mathbf{k}+\mathbf{Q}} = \xi_{\mathbf{k}}^- \xi_{\mathbf{k}+\mathbf{Q}}^- v \quad (2.15)$$

is now the breaking symmetry field, $\xi_{\mathbf{k}}^-$ are the amplitudes of the d -hole state in the quasiparticle state of energy $\varepsilon_{\mathbf{k}}^-$,

$$\xi_{\mathbf{k}}^- = \frac{V_{\mathbf{k}}}{[(\varepsilon_{d, \text{HF}} - \varepsilon_{\mathbf{k}}^-)^2 + V_{\mathbf{k}}^2]}, \quad (2.16)$$

and $c_{\mathbf{k}, \sigma}^\dagger$ are the respective creation operators. This approximation turns out to be quite satisfactory if the magnetic moment m is small, since then the approximate d -hole weights $\xi_{\mathbf{k}}^-$ in the Bloch state of energy $\varepsilon_{\mathbf{k}}^-$ do not deviate significantly from the exact ones. In addition, the entire d -hole weight concentrates in the bonding subband if $U \ll D$, so this approximation is then correct even for larger moments.

By diagonalizing the Hamiltonian H_0^- and by making projections of the quasiparticle states on the atomic states, one finds that the magnetic moment per one $3d$ orbital is given by

$$m = \frac{1}{N} \sum_{\mathbf{k}} \frac{4\xi_{\mathbf{k}}^- \xi_{\mathbf{k}+\mathbf{Q}}^- \tilde{v}_{\mathbf{k}, \mathbf{k}+\mathbf{Q}}}{[(\varepsilon_{\mathbf{k}+\mathbf{Q}}^- - \varepsilon_{\mathbf{k}}^-)^2 + 4\tilde{v}_{\mathbf{k}, \mathbf{k}+\mathbf{Q}}^2]^{1/2}}; \quad (2.17)$$

Eq. (2.17) may be further simplified by ignoring the \mathbf{k} dependence of the amplitudes and using $\xi_{\mathbf{k}}^- \approx \langle n_d \rangle^{1/2}$. By minimizing the energy

$$E_0^- = \frac{1}{L} \langle H_0^- \rangle + v \langle n_d \rangle + m + \frac{1}{4} U (\langle n_d \rangle^2 - m^2), \quad (2.18)$$

and by making use of the identity

$$\frac{\partial \langle H_0^- \rangle}{\partial \tilde{v}} = - \frac{m}{\langle n_d \rangle}, \quad (2.19)$$

one finds that the average alternating potential \tilde{v} is

$$\tilde{v} = \frac{1}{2} U \langle n_d \rangle m. \quad (2.20)$$

Therefore, the product $U \langle n_d \rangle$ plays the role of an *effective* Stoner parameter,

$$I_{\text{eff}} = U \langle n_d \rangle, \quad (2.21)$$

in the one-band model given by Eq. (2.14). The AF gap is also renormalized accordingly:

$$\Delta = U \langle n_d \rangle m. \quad (2.22)$$

Equations (2.21) and (2.22) reduce to those resulting from the single-band Hubbard model at $\langle n_d \rangle = 1$. For small values of $\langle n_d \rangle$ Eq. (2.21) is clearly an unphysical result. It is expected that at sufficiently low hole density the correlations vanish and, accordingly, the tendency towards magnetism for arbitrary large U should be suppressed. The reason is that the probability for finding two holes on the same atom in a single-particle wave function goes quickly to zero for decreasing $\langle n_d \rangle$ and this aspect is not present in HFA, leading to the linear relationship between U and I . We will show in Sec. III that the GA behaves better in this respect.

As is well known, the HFA behaves quite reasonably in the localized limit, i.e., for $\langle n_d \rangle \approx m \approx 1$, at least if the system is half filled. For instance, from Eq. (2.12) we find for the gap

$$\Delta_{\text{CT}}(m \approx 1) = D[1 + (2V/D)^2], \quad (2.23a)$$

and

$$\Delta_{\text{MH}}(m \approx 1) = U[1 - (2V/D)^2], \quad (2.23b)$$

for the CT and MH antiferromagnet, i.e., for $U > D$ and $D > U$, respectively. Thus, HFA gives the correct^{30,31} behavior of the gap. Also, the superexchange can be determined in this limit using HFA, as shown long ago by Anderson.³³ His procedure is straightforwardly generalized for the present two-band model. Let us consider a CuO_2 plane of L sites with $V \ll D$ and $V \ll U$. Under these assumptions the holes localize on Cu atoms and the AF ground state consists of two sublattices A and B of \uparrow and \downarrow spins, respectively,

$$|\Phi_{\text{AF}}\rangle = \prod_{n \in A}^{L/2} \chi_{n, \uparrow}^\dagger \prod_{m \in B}^{L/2} \chi_{m, \downarrow}^\dagger |0\rangle, \quad (2.24)$$

where $\chi_{i\sigma}^\dagger$ are the creation operators of the localized states. For convenience we perform the calculation for a 1D system; the generalization to the CuO_2 plane is straightforward. Thus we write

$$\chi_{i, \sigma}^\dagger = d_{i\sigma}^\dagger + \alpha (a_{i-1/2, \sigma}^\dagger + a_{i+1/2, \sigma}^\dagger) + \beta (d_{i-1, \sigma}^\dagger + d_{i+1, \sigma}^\dagger). \quad (2.25)$$

The energy of the state (2.24) is given by

$$E(\text{AF}) = \left\{ \varepsilon_d \sum_{\sigma} \langle d_{0\sigma}^\dagger d_{0\sigma} \rangle + U \langle d_{\uparrow 0}^\dagger d_{\uparrow 0} d_{\downarrow 0}^\dagger d_{\downarrow 0} \rangle + 4V \langle d_{\uparrow 0}^\dagger a_{1/2, \uparrow} \rangle + 4V \langle d_{\downarrow 0}^\dagger a_{1/2, \downarrow} \rangle \right\} \langle \Phi_{\text{AF}} | \Phi_{\text{AF}} \rangle^{-1}, \quad (2.26)$$

where we have chosen the reference site at $i=0$. We compare it with the energy of the F state in the localized limit,

$$|\Phi_F\rangle = \prod_{n=1}^L \chi_{n,1}^\dagger |0\rangle, \quad (2.27)$$

given by

$$E(F) = (\varepsilon_d \langle d_{0\uparrow}^\dagger d_{0\uparrow} \rangle + 4V \langle d_{0\uparrow}^\dagger a_{1/2,\uparrow} \rangle) \langle \Phi_F | \Phi_F \rangle^{-1}. \quad (2.28)$$

The values of the amplitudes α and β in Eq. (2.25) follow

$$E(AF) = \varepsilon_d \left[1 - 2 \left(\frac{V}{D} \right)^2 + 2 \left(\frac{V}{D} \right)^4 \right] - 4 \frac{V^2}{D} \left[1 - 2 \left(\frac{V}{D} \right)^2 \right] - \frac{2V^2}{D^2} \left(\frac{1}{D} + \frac{1}{U} \right), \quad (2.30)$$

and

$$E(F) = \varepsilon_d \left[1 - 2 \left(\frac{V}{D} \right)^2 + 2 \left(\frac{V}{D} \right)^4 \right] - 4 \frac{V^2}{D} \left[1 - 2 \left(\frac{V}{D} \right)^2 \right]. \quad (2.31)$$

The superexchange interaction constant has, therefore, the following form

$$J = E(F) - E(AF) = \frac{2V^4}{D^2} \left(\frac{1}{D} + \frac{1}{U} \right). \quad (2.32)$$

This formula can also be derived from many-body approaches;^{31,32} the only difference is that in HFA the system is mapped onto a classical Heisenberg spin system, because the HFA order parameter is a scalar quantity, and in a many-body approach a quantum spin Heisenberg Hamiltonian is obtained. Thus, except for the neglect of the quantum zero spin motion of the spins, HFA gives a proper description of the strong-coupling limit, because the double occupancy is projected out automatically in the completely polarized state.

III. GUTZWILLER ANSATZ AND EFFECTIVE HAMILTONIAN

A mean-field theory in the case of strong correlations may be constructed by using the GA.⁴² In the case of our Hamiltonian (2.1), the correlated wave function $|\psi_0\rangle$ is obtained from the uncorrelated one $|\phi_0\rangle$ by optimizing the number of doubly occupied $d_{x^2-y^2}$ orbitals,

$$|\psi_0\rangle = \prod_i [1 - (1-g)d_i^\dagger d_{i1} d_i^\dagger d_{i1}] |\phi_0\rangle, \quad (3.1)$$

in an analogous way as for the Anderson lattice model.⁴³⁻⁴⁶ Here we generalize the treatment of the Anderson lattice model by applying the projection operators $[1 - (1-g)n_{i\uparrow}n_{i\downarrow}]$ to the HF states $|\phi_0\rangle$ having AF long-range order. We believe that, similarly as for the single-band model,⁴⁷ a sensible description of the correlated regime may be obtained in this way.

The evaluation of the correlated wave function is not possible without further approximations. We have adopted a Gutzwiller approximation to evaluate the energy

from the level structure of the considered localized system in the HFA,

$$\alpha = -\frac{V}{D}, \quad (2.29a)$$

$$\beta = \frac{V^2}{DU}. \quad (2.29b)$$

In the F case one finds as well $\alpha = -V/D$, but $\beta = 0$. These coefficients are next used to calculate the correlation functions in Eqs. (2.26) and (2.28). One finds that

which reduces the problem to simple combinatorics on a lattice.⁴⁸ Since the projection operators refer only to the correlated d orbitals in our case, the normalization of the wave function may be written as follows:

$$\langle \psi_0 | \psi_0 \rangle = \sum_D g^{2D} N_D(L, N_\uparrow, N_\downarrow) P(L, N_\uparrow) P(L, N_\downarrow). \quad (3.2)$$

Here

$$N_D(L, N_\uparrow, N_\downarrow) = C_{N_\uparrow}^L C_D^{N_\downarrow} C_{N_\uparrow - D}^{L - N_\downarrow} \quad (3.3)$$

is the number of combinations to distribute the holes over the lattice of L available sites. N_σ is the number of σ -spin holes, while D stands for the total number of doubly occupied sites. The probability factors

$$P(L, N_\sigma) = n_\sigma^{N_\sigma} (1 - n_\sigma)^{L - N_\sigma}, \quad (3.4)$$

where $n_\sigma = N_\sigma/L$, follow from the binomial distribution. Similarly as for the Hubbard model,⁴⁷ we use the largest-term approximation, valid in the thermodynamic limit. It gives the relation between the variational parameter g and the fraction of doubly occupied sites $d = D/L$,

$$g^2 = \frac{d(1 - n_d + d)}{(n_\uparrow - d)(n_\downarrow - d)}, \quad (3.5)$$

when applied to Eq. (3.2). Here we use the simplified notation $n_d = \langle n_d \rangle$.

For our model Hamiltonian, which has a tight-binding form, the evaluation of the kinetic energy by using the Gutzwiller approximation is straightforward. Let us consider the possible elemental processes that contribute to the kinetic energy (shown schematically in Fig. 1). They describe a hole propagating either away or to a given site i . We evaluate the probabilities of each of them by treating all distributions of electrons at the lattice as independent. This scheme is well known and has been applied before to a single magnetic impurity,⁴⁹ the Hubbard Hamiltonian,⁴⁸ as well as to the Anderson lattice.⁴³⁻⁴⁶ Therefore, we present here only the outline of the actual calculation and refer the reader to the existing literature for more details.

For the processes in which a σ hole moves away from the considered d orbital [see Figs. 1(a) and 1(b)], the probability of each configuration is described by a combinatorial expression analogous to Eq. (3.2). The

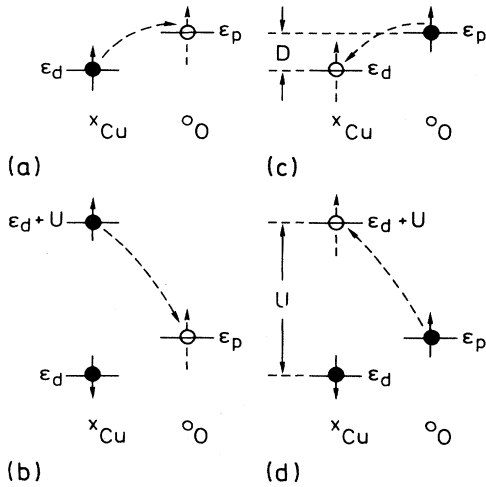


FIG. 1. Schematic transitions between neighboring Cu and O atoms in a CuO_2 lattice which contribute to the kinetic energy: (a), (b), (c), and (d) for d hole moving away and coming to the considered Cu site, respectively.

differences are as follows: (i) the number of available lattice sites available for other holes not involved in the considered hopping process is reduced by one, and (ii) the number of N_σ holes is also reduced by one. The resulting expression for the hopping term has to be normalized by the norm (3.2) and the result is

$$\frac{\langle \psi_0 | a_{m\sigma}^\dagger d_{i\sigma} | \psi_0 \rangle^{(a)}}{\langle \psi_0 | \psi_0 \rangle} = \frac{1}{n_{i\sigma}} (n_{i\sigma} - d) \langle \phi_0 | a_{m\sigma}^\dagger d_{i\sigma} | \phi_0 \rangle, \quad (3.6a)$$

and

$$\frac{\langle \psi_0 | a_{m\sigma}^\dagger d_{i\sigma} | \psi_0 \rangle^{(b)}}{\langle \psi_0 | \psi_0 \rangle} = \frac{1}{n_{i\sigma}} g \frac{(n_{i\uparrow} - d)(n_{i\downarrow} - d)}{(1 - n_d + d)} \times \langle \phi_0 | a_{m\sigma}^\dagger d_{i\sigma} | \phi_0 \rangle, \quad (3.6b)$$

where (a) and (b) refer to the transitions of Figs. 1(a) and 1(b), respectively. We assumed in Eqs. (3.6a) and (3.6b) that the average double occupancy at site i is just given by an average quantity d which is the case for the considered AF order. By adding the two terms (3.6a) and (3.6b) we get the renormalization factor for the kinetic energy processes which describe the hole propagating away from the considered site,

$$q_{i\sigma}^{(1)} = \frac{1}{n_{i\sigma}} \left[(n_{i\sigma} - d) + g \frac{(n_{i\uparrow} - d)(n_{i\downarrow} - d)}{(1 - n_d + d)} \right]. \quad (3.7)$$

Effectively, it means that instead of calculating the kinetic energy explicitly by using the correlated wave function, we may use the prescription that

$$\frac{\langle \psi_0 | a_{m\sigma}^\dagger d_{i\sigma} | \psi_0 \rangle}{\langle \psi_0 | \psi_0 \rangle} = q_{i\sigma}^{(1)} \langle \phi_0 | a_{m\sigma}^\dagger d_{i\sigma} | \phi_0 \rangle, \quad (3.8)$$

$$E_0 = \frac{1}{L} \langle \psi_0 | \sum_{i,\sigma} (\epsilon_d - \mu_{i\sigma}) d_{i\sigma}^\dagger d_{i\sigma} + \epsilon_p \sum_{m,\sigma} a_{m\sigma}^\dagger a_{m\sigma} + U \sum_i d_{i\uparrow}^\dagger d_{i\uparrow} d_{i\downarrow}^\dagger d_{i\downarrow} + V \sum_{\langle i,m \rangle \sigma} (d_{i\sigma}^\dagger a_{m\sigma} + \text{H.c.}) + \sum_{i,\sigma} \mu_{i\sigma} d_{i\sigma}^\dagger d_{i\sigma} | \psi_0 \rangle \langle \psi_0 | \psi_0 \rangle^{-1}. \quad (3.16)$$

In an analogous way we find that

$$\frac{\langle \psi_0 | d_{i\sigma}^\dagger a_{m\sigma} | \psi_0 \rangle^{(c)}}{\langle \psi_0 | \psi_0 \rangle} = \frac{1}{(1 - n_{i\sigma})} (1 - n_d + d) \times \langle \phi_0 | d_{i\sigma}^\dagger a_{m\sigma} | \phi_0 \rangle. \quad (3.9a)$$

and

$$\frac{\langle \psi_0 | d_{i\sigma}^\dagger a_{m\sigma} | \psi_0 \rangle^{(d)}}{\langle \psi_0 | \psi_0 \rangle} = \frac{1}{(1 - n_{i\sigma})} g (n_{i,-\sigma} - d) \times \langle \phi_0 | d_{i\sigma}^\dagger a_{m\sigma} | \phi_0 \rangle, \quad (3.9b)$$

for the processes shown in Figs. 1(c) and 1(d), respectively. The renormalization factor for the hole propagating to the considered site is, therefore, given by

$$q_{i\sigma}^{(2)} = \frac{1}{(1 - n_{i\sigma})} [(1 - n_d + d) + g (n_{i,-\sigma} - d)]. \quad (3.10)$$

It has a similar meaning to $q_{i\sigma}^{(1)}$, i.e.,

$$\frac{\langle \psi_0 | d_{i\sigma}^\dagger a_{m\sigma} | \psi_0 \rangle}{\langle \psi_0 | \psi_0 \rangle} = q_{i\sigma}^{(2)} \langle \phi_0 | d_{i\sigma}^\dagger a_{m\sigma} | \phi_0 \rangle. \quad (3.11)$$

Since both types of processes appear always pairwise when the energy is evaluated, the kinetic energy is renormalized by their product

$$q_{i\sigma} = q_{i\sigma}^{(1)} q_{i\sigma}^{(2)}. \quad (3.12)$$

By making use of Eq. (3.5), the renormalization factor $q_{i\sigma}$ may be explicitly written as follows:

$$q_{i\sigma} = \frac{1}{n_{i\sigma}(1 - n_{i\sigma})} \{ [(1 - n_d + d)(n_{i\sigma} - d)]^{1/2} + [d(n_d - n_{i\sigma} - d)]^{1/2} \}^2. \quad (3.13)$$

It gives the well-known expression $q_{i\sigma} = [(1 - n_d)/(1 - n_{i\sigma})]$ at $U = \infty$.⁴³

Instead of considering the original Hamiltonian (2.1) and calculating the energy with the correlated wave function (3.1), we may now use an effective Hamiltonian

$$H_{\text{eff}} = \sum_{i,\sigma} (\epsilon_d - \mu_{i\sigma}) d_{i\sigma}^\dagger d_{i\sigma} + \epsilon_p \sum_{m,\sigma} a_{m\sigma}^\dagger a_{m\sigma} + \sum_{\langle i,m \rangle \sigma} V_{i\sigma} (d_{i\sigma}^\dagger a_{m\sigma} + \text{H.c.}), \quad (3.14)$$

where the original hybridization element V has been replaced by the renormalized one,

$$V \rightarrow V_{i\sigma} = q_{i\sigma}^{1/2} V. \quad (3.15)$$

Thus, we find the same renormalization factor for the hybridization element as for the Anderson lattice problem⁴³⁻⁴⁶ and for the Hubbard model.^{42,48} The quantities $\mu_{i\sigma}$ are the chemical potentials to optimize the densities of d holes in the correlated state, as first introduced by Rice and Ueda.⁴³ The energy of the system is calculated by minimizing the energy

By making use of the Gutzwiller approximation, it may be written in the following form:

$$E_0 = \frac{1}{L} \langle H_{\text{eff}} \rangle + Ud + \frac{1}{L} \sum_{i,\sigma} \mu_{i\sigma} \langle d_{i\sigma}^\dagger d_{i\sigma} \rangle, \quad (3.17)$$

where $d = \langle d_{i1}^\dagger d_{i1} d_{i2}^\dagger d_{i2} \rangle$. Equation (3.17) has to be minimized with respect to the variational parameters $\{\mu_{i1}, \mu_{i2}, d\}$. This approximate procedure is known to approximate very well the result of the rigorous treatment of the variational problem for the Anderson lattice within the GA in the NM and F case.⁴⁵ Therefore, we believe that the present approach describes correctly the physical properties of AF phase on the mean-field level. It includes the essential ingredients of a strongly correlated system: (i) optimization with respect to the average number of doubly occupied sites d , and (ii) redistribution of charge in presence of correlations. In the Appendix we show that when this procedure is applied to the Hamiltonian (3.14) it reproduces the exact ground-state energy for a cluster consisting of one Cu atom surrounded by four oxygen atoms and filled by two holes. This shows that the GA is an excellent approximation on this smallest, nontrivial length scale. In this context we also note that the GA reproduces the correct Kondo exponent in the single Anderson impurity problem.⁵⁰

The structure of H_{eff} is to some extent similar to that of

$$H_{\text{eff}} = \sum_{\mathbf{k},\sigma} \begin{pmatrix} \bar{\epsilon}_d & \bar{V}_{\mathbf{k}} & \bar{v} & \delta_{\mathbf{k}} \\ \bar{V}_{\mathbf{k}} & \epsilon_p & \delta_{\mathbf{k}+\mathbf{Q}} & 0 \\ \bar{v} & \delta_{\mathbf{k}+\mathbf{Q}} & \bar{\epsilon}_d & \bar{V}_{\mathbf{k}+\mathbf{Q}} \\ \delta_{\mathbf{k}} & 0 & \bar{V}_{\mathbf{k}+\mathbf{Q}} & \epsilon_p \end{pmatrix} \begin{pmatrix} d_{\mathbf{k},\sigma} \\ a_{\mathbf{k},\sigma} \\ d_{\mathbf{k}+\mathbf{Q},\sigma} \\ a_{\mathbf{k}+\mathbf{Q},\sigma} \end{pmatrix}, \quad (3.23)$$

where the elements $\bar{V}_{\mathbf{k}}$ and $\delta_{\mathbf{k}}$ are defined as follows:

$$\bar{V}_{\mathbf{k}} = \bar{V} \gamma_{\mathbf{k}}, \quad (3.24)$$

$$\delta_{\mathbf{k}} = \delta \gamma_{\mathbf{k}}. \quad (3.25)$$

The structure of the 4×4 matrix in Eq. (3.23) is changed as compared with that of Eq. (2.4) due to the alternation in renormalized hybridization elements $V_{i\sigma}$ which is expressed by the presence of elements $\delta_{\mathbf{k}}$ on the antidiagonal. Therefore, one cannot, in general, find an analytic expression for the AF gap to compare with Eq. (2.12) and the GA solution cannot be mapped exactly on a Stoner theory for arbitrary parameters.

As we will now show, such a mapping is possible for small $\langle n_d \rangle$ or either m . In contrast to HFA, a true weak-coupling behavior for arbitrary U is found in this limit, and we will derive the effective Stoner parameter. In the NM case (i.e., at $\bar{v} = 0$ and $\delta_{\mathbf{k}} = 0$), the solution of Eq. (3.23) is obtained by applying a canonical transformation analogous to that of Eq. (2.6):

$$\begin{pmatrix} \bar{a}_{\mathbf{k},\sigma} \\ \bar{\beta}_{\mathbf{k},\sigma} \end{pmatrix} = \begin{pmatrix} \bar{\xi}_{\mathbf{k}} & \bar{\zeta}_{\mathbf{k}} \\ -\bar{\zeta}_{\mathbf{k}} & \bar{\xi}_{\mathbf{k}} \end{pmatrix} \begin{pmatrix} d_{\mathbf{k},\sigma} \\ a_{\mathbf{k},\sigma} \end{pmatrix}. \quad (3.26)$$

The resulting bonding and antibonding states are

$$\bar{\epsilon}_{\mathbf{k}}^\pm = \frac{1}{2} (\epsilon_p + \bar{\epsilon}_d) \pm \frac{1}{2} [(\epsilon_p - \bar{\epsilon}_d)^2 + 4\bar{V}_{\mathbf{k}}^2]^{1/2}. \quad (3.27)$$

H_0 . Now the d -hole level is renormalized to

$$\bar{\epsilon}_d = \epsilon_d - \mu \quad (3.18)$$

from the atomic value ϵ_d by the average potential

$$\mu = \frac{1}{2} (\mu_{01} + \mu_{02}). \quad (3.19)$$

The difference between the chemical potentials,

$$\bar{v} = \frac{1}{2} (\mu_{01} - \mu_{02}), \quad (3.20)$$

where $i=0$ is the reference site, determines the alternating potential, analogous to that of the HFA. The new feature of the present effective Hamiltonian H_{eff} is the renormalization of the hybridization element $V_{i\sigma}$. It depends on the actual density $n_{i\sigma}$ at the site i at which it acts. Therefore, in an AF lattice, the hybridization $V_{i\sigma}$ changes from one sublattice to the other, following the changes of the magnetic moment. It is convenient to define the average hybridization element

$$\bar{V} = \frac{1}{2} (V_{01} + V_{02}) \quad (3.21)$$

and the difference in the hybridization

$$\delta = \frac{1}{2} (V_{01} - V_{02}). \quad (3.22)$$

Our Hamiltonian (3.14) may now be Fourier transformed to the form

Similarly, as in the HFA, one may consider again a simplified problem of the AF order which results from the magnetic coupling within the bonding subband $\bar{\epsilon}_{\mathbf{k}}^-$ in GA. In this case, one gets from Eq. (3.23),

$$H_{\text{eff}}^- = \sum_{\mathbf{k},\sigma} (c_{\mathbf{k},\sigma}^\dagger c_{\mathbf{k}+\mathbf{Q},\sigma}^\dagger) \begin{pmatrix} \bar{\epsilon}_{\mathbf{k}}^- & \bar{v}_{\mathbf{k},\mathbf{k}+\mathbf{Q}} \\ \bar{v}_{\mathbf{k},\mathbf{k}+\mathbf{Q}} & \bar{\epsilon}_{\mathbf{k}+\mathbf{Q}}^- \end{pmatrix} \begin{pmatrix} c_{\mathbf{k},\sigma} \\ c_{\mathbf{k}+\mathbf{Q},\sigma} \end{pmatrix}, \quad (3.28)$$

where

$$\bar{v}_{\mathbf{k},\mathbf{k}+\mathbf{Q}} = \bar{\xi}_{\mathbf{k}}^- \bar{\xi}_{\mathbf{k}+\mathbf{Q}}^- \bar{v} + \bar{\xi}_{\mathbf{k}}^- \bar{\zeta}_{\mathbf{k}+\mathbf{Q}}^- \delta_{\mathbf{k}+\mathbf{Q}} + \bar{\xi}_{\mathbf{k}+\mathbf{Q}}^- \bar{\zeta}_{\mathbf{k}}^- \delta_{\mathbf{k}} \quad (3.29)$$

is the alternating potential. $\bar{\xi}_{\mathbf{k}}^-$ and $\bar{\zeta}_{\mathbf{k}}^-$ are now the amplitudes of d - and p -hole states in the bonding state $\bar{\epsilon}_{\mathbf{k}}^-$, respectively. They are defined in an analogous way to Eq. (2.14),

$$\bar{\xi}_{\mathbf{k}}^- = \frac{\bar{V}_{\mathbf{k}}}{[(\bar{\epsilon}_d - \bar{\epsilon}_{\mathbf{k}}^-)^2 + \bar{V}_{\mathbf{k}}^2]}, \quad (3.30a)$$

$$\bar{\zeta}_{\mathbf{k}}^- = \frac{\bar{\epsilon}_d - \bar{\epsilon}_{\mathbf{k}}^-}{[(\bar{\epsilon}_d - \bar{\epsilon}_{\mathbf{k}}^-)^2 + \bar{V}_{\mathbf{k}}^2]}, \quad (3.30b)$$

in terms of the renormalized parameters. After a self-

consistent solution one may find the magnetic moment

$$m = \frac{1}{N} \sum_{\mathbf{k}} \frac{4\bar{\xi}_{\mathbf{k}}^- \bar{\xi}_{\mathbf{k}+\mathbf{Q}}^- \bar{v}_{\mathbf{k},\mathbf{k}+\mathbf{Q}}}{[(\bar{\delta}_{\mathbf{k}+\mathbf{Q}}^- - \bar{\delta}_{\mathbf{k}}^-)^2 + 4\bar{v}_{\mathbf{k},\mathbf{k}+\mathbf{Q}}^2]^{1/2}}. \quad (3.31)$$

It is again of interest to consider the simplified problem by ignoring the \mathbf{k} dependence of the amplitudes $\bar{\xi}_{\mathbf{k}}^-$ and $\bar{\zeta}_{\mathbf{k}}^-$, i.e., assuming $\bar{\xi}_{\mathbf{k}}^- \approx \langle n_d \rangle^{1/2}$ and $\bar{\zeta}_{\mathbf{k}}^- \approx \langle 1 - n_d \rangle^{1/2}$. In addition, we replace the elements $\delta_{\mathbf{k}}$ in Eq. (3.29) by the average quantities, introducing

$$\gamma_0 = \frac{1}{L} \sum_{\mathbf{k}} \gamma_{\mathbf{k}}. \quad (3.32)$$

Under this approximation one finds the following formula for the average potential that breaks the magnetic symmetry:

$$\bar{v} = \langle n_d \rangle \bar{v} + 2\gamma_0 \langle n_d \rangle \langle 1 - n_d \rangle^{1/2} \delta. \quad (3.33)$$

In order to express it by the parameters of the model Hamiltonian we minimize the energy

$$E_0^- = \frac{1}{L} \langle H_{\text{eff}}^- \rangle + \bar{v} \langle n_d \rangle + m + Ud \quad (3.34)$$

with respect to \bar{v} . By making use of the identity

$$\frac{\partial \langle H_{\text{eff}}^- \rangle}{\partial \bar{v}} = - \frac{m}{\langle n_d \rangle}, \quad (3.35)$$

and by replacing the derivatives over \bar{v} by the derivatives over m , one finds that

$$\bar{v} = -U \langle n_d \rangle \left[\frac{\partial d}{\partial m} \right] + 2\gamma_0 [\langle n_d \rangle \langle 1 - n_d \rangle]^{1/2} \left[\delta + m \left[\frac{\partial \delta}{\partial m} \right] \right]. \quad (3.36)$$

If one neglects electron correlation, i.e., assumes that $d = \frac{1}{4} (\langle n_d \rangle^2 - m^2)$ and neglects the second term in Eq. (3.36) which results from the alternation in the effective hybridization element $V_{i\sigma}$, Eq. (3.36) reproduces the result of the HFA given in Eq. (2.21).

In order to evaluate the effective potential \bar{v} as given in Eq. (3.36), one needs to know (i) the explicit dependence of d on m , and (ii) the value of $\delta + m(\partial\delta/\partial m)$. Let us determine first the double occupancy d . By requiring that the energy functional (3.17) is stationary with respect to d , one finds that

$$U + V \sum_{\sigma} q_{0\sigma}^{1/2} \left[\frac{\partial \ln q_{0\sigma}}{\partial d} \right] \frac{1}{L} \sum_{\mathbf{k}} \gamma_{\mathbf{k}} \bar{\xi}_{\mathbf{k}}^- \bar{\zeta}_{\mathbf{k}}^- = 0, \quad (3.37)$$

which may be further simplified to

$$U - (\langle n_d \rangle \langle 1 - n_d \rangle)^{1/2} \gamma_0 V \sum_{\sigma} q_{0\sigma}^{1/2} \left[\frac{\partial \ln q_{0\sigma}}{\partial d} \right] = 0 \quad (3.38)$$

by making the same approximations as in the derivation of Eq. (3.33). The above condition (3.37) corresponds to Eq. (3.27) of Vulović and Abrahams⁴⁶ given for the NM or F Anderson lattice. Since the analytic solution of (3.38) is not possible for arbitrary values of U , we consider only $U \gg V$, where the Stoner parameter as obtained in the HFA (2.19) is overestimated. In this limit of $d \approx 0$

and for $m \approx 0$, the Gutzwiller renormalization factors are

$$q_{0\sigma} = \frac{1 - \langle n_d \rangle}{1 - \frac{1}{2} \langle n_d \rangle} \left[1 \pm \frac{m}{1 - \frac{1}{2} \langle n_d \rangle} \right]. \quad (3.39)$$

By evaluating the leading contribution to the derivative ($\partial q_{0\sigma} / \partial d$) and using Eq. (3.38), we find that

$$d = 4 \left[\frac{\gamma_0 V}{U} \right]^2 \frac{\langle 1 - n_d \rangle}{\langle n_d \rangle (1 - \frac{1}{2} \langle n_d \rangle)} (\langle n_d \rangle^2 - m^2). \quad (3.40)$$

This shows that the applied approximation scheme is correct in the strongly correlated regime, where the double occupancy d is excited only in virtual transitions to the higher-energy states and is thus expected to be proportional to $(V/U)^2$. From Eq. (3.40) one finds that

$$\left[\frac{\partial d}{\partial m} \right] = -2 \left[\frac{\gamma_0 V}{U} \right]^2 \frac{\langle 1 - n_d \rangle}{\langle n_d \rangle (1 - \frac{1}{2} \langle n_d \rangle)} m. \quad (3.41)$$

Furthermore, if $d \approx 0$ and $m \approx 0$,

$$\delta + m \left[\frac{\partial \delta}{\partial m} \right] = \frac{1}{2} V \frac{(1 - \langle n_d \rangle)^{1/2}}{(1 - \frac{1}{2} \langle n_d \rangle)^{3/2}} m. \quad (3.42)$$

The symmetry-breaking field \bar{v} is now found by inserting Eqs. (3.41) and (3.42) into Eq. (3.33),

$$\bar{v} = \gamma_0 V \frac{1 - \langle n_d \rangle}{1 - \frac{1}{2} \langle n_d \rangle} \left[\left[\frac{\langle n_d \rangle}{1 - \frac{1}{2} \langle n_d \rangle} \right]^{1/2} + 2 \frac{\gamma_0 V}{U} \right] m. \quad (3.43)$$

This results in the effective Stoner parameter for the considered single-band (bonding state) problem,

$$\bar{I}_{\text{eff}} = \gamma_0 V \frac{1 - \langle n_d \rangle}{1 - \frac{1}{2} \langle n_d \rangle} \left[\frac{1}{2} \left[\frac{\langle n_d \rangle}{1 - \frac{1}{2} \langle n_d \rangle} \right]^{1/2} + \frac{\gamma_0 V}{U} \right]. \quad (3.44)$$

For $U \rightarrow \infty$, we find

$$\bar{I}_{\text{eff}}^{\infty} = \frac{1}{2} \gamma_0 V (1 - \langle n_d \rangle) \frac{\langle n_d \rangle^{1/2}}{(1 - \frac{1}{2} \langle n_d \rangle)^{3/2}}. \quad (3.45)$$

Equations (3.44) and (3.45) are the central results of this section. They show that from the GA a description for the magnetism is obtained which is at least in a qualitative sense correct. For U larger than the bandwidth, this quantity should give only a correction to I_{eff} and we find indeed that U enters Eq. (3.44) in a strong-coupling form. In contrast to the HFA result Eq. (2.21), the scale for I_{eff} is set by the hybridization, as it should be, and I_{eff} is proportional to $\langle n_d \rangle^{1/2}$ for small $\langle n_d \rangle$. Opposite to the HFA result Eq. (2.21), it follows from Eq. (3.44) that a *decreasing* U gives rise to an *increasing* I_{eff} , reflecting the strong-coupling way in which U enters the weak-coupling problem.

Let us now turn to the localized limit and consider again the bonding hole subband $\bar{\alpha}_{\mathbf{k}}^-$. It is expected that GA reduces here to HFA, because of the proper description obtained from the latter approximation. This is indeed what we find. The similarity between both theories can already be seen by comparing the magnitude of the gap. In the strongly magnetic limit, i.e., for $m \approx \langle n_d \rangle$, one

finds that

$$\bar{\Delta} = (\mu_{0\uparrow} - \mu_{0\downarrow}) \langle n_d \rangle + 4\gamma_0 V [\langle n_d \rangle (1 - n_d)]^{1/2} \delta. \quad (3.46)$$

Of course, the gap $\bar{\Delta}$ does not equal to the product $I_{\text{eff}} m$, since the effective Stoner parameter I_{eff} derived above is valid only for $m \rightarrow 0$. The second term is only a correction to the first one if $V \ll \bar{v}$ (or $V \ll U$). This shows that the difference between the chemical potentials $\mu_{i\sigma}$ is now playing an analogous role to the Coulomb interaction U in the HFA and the gap value is renormalized by the hole density $\langle n_d \rangle$, as in the HFA [see Eq. (2.22)].

The direct correspondence between GA and HFA in the localized limit can be shown explicitly by considering the superexchange. For that purpose, let us use the localized states analogous to those given in Eqs. (2.24) and (2.27). In the AF case we have

$$|\Psi_{\text{AF}}\rangle = \prod_{n \in A}^{L/2} \bar{\chi}_{n,\uparrow}^\dagger \prod_{m \in B}^{L/2} \bar{\chi}_{m,\downarrow}^\dagger |0\rangle, \quad (3.47)$$

$$\bar{E}(\text{AF}) = \varepsilon_d \left[1 - 2 \left(\frac{V_{0\uparrow}}{\Delta_1} \right)^2 + 2 \left(\frac{V_{0\uparrow}}{\Delta_1} \right)^4 \right] + Ud - 4 \frac{V_{0\uparrow}^2}{\Delta_1} \left[1 - 2 \left(\frac{V_{0\uparrow}}{\Delta_1} \right)^2 \right] - 2 \frac{V_{0\uparrow}^4}{\Delta_1^3} - 4 \frac{V_{0\downarrow}^2}{\Delta_2} \left(\frac{V_{0\uparrow}}{\Delta_1} \right)^2. \quad (3.50)$$

It has to be minimized with respect to the variational parameters $\{\Delta_1, \Delta_2, d\}$. One finds that the renormalization factors of the hybridization elements $V_{0\sigma}$ are given by

$$q_{0\uparrow} = 1 + 2 \left(\frac{V}{\Delta_1} \right)^2, \quad (3.51a)$$

$$q_{0\downarrow} = \left(\frac{d}{2} \right)^{1/2} \left(\frac{V^2}{\Delta_1 \Delta_2} \right)^{-1/2}, \quad (3.51b)$$

up to the terms of order V^2 . By using Eq. (3.51b) one

$$\bar{E}(\text{AF}) = \varepsilon_d \left[1 - 2 \left(\frac{V}{D} \right)^2 + 2 \left(\frac{V}{D} \right)^4 \right] - 4 \frac{V^2}{D} \left[1 - 2 \left(\frac{V}{D} \right)^2 \right] - 2 \frac{V^2}{D^2} \left(\frac{1}{D} + \frac{1}{U} \right). \quad (3.53)$$

We compare $\bar{E}(\text{AF})$ with the energy of the F state $\bar{E}(F)$ in the localized limit

$$|\Psi_F\rangle = \prod_{n=1}^L \bar{\chi}_{n,\uparrow}^\dagger |0\rangle. \quad (3.54)$$

The energy may be evaluated in an analogous way as in Eq. (2.27) to give

$$\bar{E}(F) = \varepsilon_d \left[1 - 2 \left(\frac{V_{0\uparrow}}{\Delta_1} \right)^2 + 2 \left(\frac{V_{0\uparrow}}{\Delta_1} \right)^4 \right] - 4 \frac{V_{0\uparrow}^2}{\Delta_1} \left[1 - 2 \left(\frac{V_{0\uparrow}}{\Delta_1} \right)^2 \right]. \quad (3.55)$$

The minimization procedure in the leading order again gives the same result as in Eq. (3.52a), and

$$\bar{E}(F) = \varepsilon_d \left[1 - 2 \left(\frac{V}{D} \right)^2 + 2 \left(\frac{V}{D} \right)^4 \right] - 4 \frac{V^2}{D} \left[1 - 2 \left(\frac{V}{D} \right)^2 \right]. \quad (3.56)$$

where $\bar{\chi}_{i\sigma}^\dagger$ are the creation operators of the localized states in the GA. In the case of a 1D chain they read

$$\bar{\chi}_{i,\sigma}^\dagger = d_{i\sigma}^\dagger + \bar{\alpha} (a_{i-1/2,\sigma}^\dagger + a_{i+1/2,\sigma}^\dagger) \bar{\beta} (d_{i-1,\sigma}^\dagger + d_{i+1,\sigma}^\dagger), \quad (3.48)$$

and the amplitudes are

$$\bar{\alpha} = - \frac{V_{0\uparrow}}{\Delta_1}, \quad (3.49a)$$

$$\bar{\beta} = \frac{V_{0\uparrow} V_{0\downarrow}}{\Delta_1 \Delta_2}, \quad (3.49b)$$

where Δ_1 and Δ_2 are the energy differences between the effective levels, to be determined variationally. The energy of the AF state, evaluated as in Eq. (2.26), is given by

may eliminate Δ_2 from Eq. (3.50) and minimize the resulting expression with respect to Δ_1 and d . As a result one finds that

$$\Delta_1 = D, \quad (3.52a)$$

$$d = 2 \left(\frac{V^2}{DU} \right)^2, \quad (3.52b)$$

in the leading order in V . By inserting Eqs. (3.52a) and (3.52b) into Eq. (3.50), we find that

By comparing the energies of AF (3.53) and F (3.56) state, one finds within the GA that the superexchange interaction is given by

$$J = \bar{E}(F) - \bar{E}(\text{AF}) = 2 \left(\frac{V^2}{D} \right)^2 \left(\frac{1}{D} + \frac{1}{U} \right) \quad (3.57)$$

which agrees with the HFA result Eq. (2.32).

In summary, we have shown in this section that in the localized limit GA and HFA are completely equivalent, both giving a correct answer as long as the spin fluctuations can be neglected. However, in the regime dominated by charge fluctuations (small $\langle n_d \rangle$), HFA is strongly in error for large U , while GA yields the sensible result that the magnetism can be described with a weak-coupling (Stoner) theory in which U appears in a strong-coupling fashion. The question of how to interpolate between these highly different situations (intermediate coupling) is the subject of Sec. IV.

IV. NUMERICAL ANALYSIS AND COMPARISON BETWEEN THE HARTREE-FOCK APPROXIMATION AND THE GUTZWILLER ANSATZ

For numerical convenience and because we expect that there is no essential dependence on the dimensionality we have chosen to evaluate the GA and HFA equations using a simplified 1D model of an alternating Cu-O chain. The unit cell consists then of one Cu and one O atom, and the band structure is given by the bonding and antibonding bands. This mimics the band structure of the perovskite planes since the nonbonding state present in a 2D band structure is always empty (i.e., contains no holes) and does not contribute to the ground-state energy. Further, both systems are unstable with respect to the AF order due to the perfect nesting property.

The bonding and antibonding states of a 1D Cu-O system are found according to the scheme described in Secs. II and III. The only difference is that the Fourier transformed hybridization elements are now of the following forms: in the HFA,

$$V_k = 2V \cos \frac{1}{2} k ; \quad (4.1)$$

by using the GA,

$$\bar{V}_k = 2\bar{V} \cos \frac{1}{2} k , \quad (4.2)$$

$$\delta_k = 2\delta \cos \frac{1}{2} k . \quad (4.3)$$

This means that we have an effective reduction of the hybridization effect by a factor of $2^{1/2}$ in 1D and, thus, the value of V in the analytic expression for the gap in the HFA, Eq. (2.12), as well as the value of γ_0 in Eqs. (3.36)–(3.46), have to be modified accordingly. The band structure which follows from the HF and GA problems is presented in Fig. 2 for an intermediate-coupling situation. The Δ 's are chosen such that the magnetic moments in the AF states found in HFA and GA are close (0.547 and 0.540, respectively), while we used the same U and V . For convenience, the band structure is shown in the conventional electronic notation. We consider the case of one hole, i.e., three electrons per unit cell of a Cu-O chain. Let us first consider the HFA bands. In the NM state, the effective d level is strongly renormalized downwards, giving rise to a strong decrease of $\langle n_d \rangle$ which is known to be, to some extent, unphysical. The AF band structure already makes more sense. One (\downarrow -spin) effective d level is renormalized upwards with respect to the NM case approaching the bare d -level position, while the other (\uparrow -spin) lies at $\approx 0.6U$ lower energy. This already starts to look like the correct picture with mixed “ d^9 - $d^{10}L$ ” bands around the Fermi energy E_F and a d^8 band at the energy lower by $\approx U$. Turning to the GA bands, we first note that the effective one electron levels appearing in this scheme lack a relationship with the true quasiparticles, because they are instrumental devices which serve to determine the correlated ground state. This becomes particularly obvious when the GA levels of the five site cluster, as analyzed in the Appendix, are compared to the true states of this system. Of course, under the neglect of self-localization effects, the gap can be deduced from the GA bands because in this case the discontinuity in the deriva-

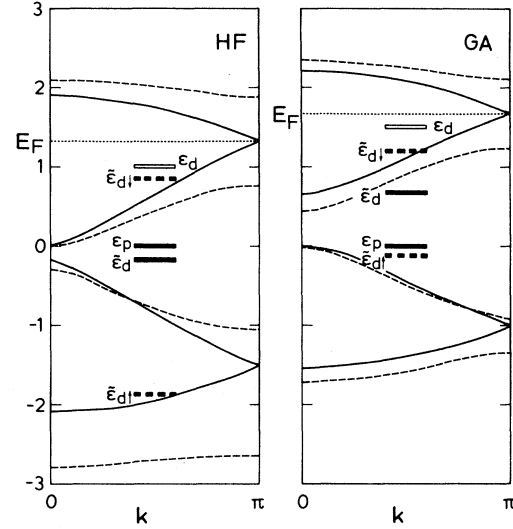


FIG. 2. One-dimensional band structure (in the units of V) in a nonmagnetic (solid lines) and antiferromagnetic (dashed lines) state for $U/V=5$ as found in the HFA (left-hand side) and by using the GA (right-hand side). We have chosen $\epsilon_p=0$ and the charge transfer energy of $D/V=1$ and 1.5 for the HFA and the GA, respectively, which gives the magnetic moment $m=0.55$. Index k refers to the band states of the *folded* Brillouin zone. Renormalized hole levels, $\tilde{\epsilon}_d$ and $\tilde{\epsilon}_{d\sigma}$ are indicated in both panels for the NM and AF cases, respectively.

tive of the thermodynamic potential to particle number coincides with the gap appearing in the GA bands.

Nevertheless, we can get some intuitive feel about the difference between the GA and HFA ground states by considering Fig. 2. In the NM state, the GA effective d level is shifted less than the HFA d level, despite the larger Δ . This indicates that, in comparison to HFA, GA favors a higher d occupancy, which we will discuss later in more detail. The GA bands are only slightly narrowed compared to the HFA bands; this is surprising in view of the d -hole count, and we suspect that the real bands are more narrowed. Turning to the AF GA bands, the most striking observation is the collapse of the splitting of the d levels, compared to the HFA case. This can be understood in the following way: For infinite U , this splitting has a limiting value D in the extremely localized regime. In fact, in Fig. 2 this splitting is already quite close to this limiting value. Because of this small splitting it still makes sense to consider only the antibonding band in so far as one is concerned with the antiferromagnetism. Using $\langle n_d \rangle = 0.66$ we obtain a gap of $0.88V$ from Eq. (3.46), in excellent agreement with the numerical gap of $0.89V$. It also follows from Eq. (3.46) that the gap is largely due to the GA d -level splitting while the spin dependence of the hopping matrix element only adds a small correction. At least in so far as the gap is considered, the GA already behaves like the HFA with renormalized parameter values.

The results for the AF gap E_{gap}/V are presented in Fig. 3. For a fixed value of U , the gap increases gradually with

the increasing value of charge transfer energy D/V , both in the HFA and in GA. A different limiting behavior is observed, depending on the values of the parameters. On one hand, for small U ($U/V=2.5$), the HF gap approaches gradually a value of U in the limit of large D , as predicted by Eq. (2.21b). It is also the case in the GA, so apparently the difference between the respective chemical potentials \bar{v} approaches there also the value of U , as suggested by our analysis of the localized limit. On the other hand, for large U ($U/V=10$) the value of the AF gap remains close to D in the HFA, starting from $D/V \approx 2$. It is even closer to the value of D in the GA. This shows again that in the latter case the value of \bar{v} is close to D which gives in this case the energy scale for the AF gap. The largest differences between the respective values of E_{gap} as found in the HFA and by using the GA are observed for $D/V \approx 0$. This is expected from the discussion in Sec. III, where we showed that HFA is incorrect for large U and small $\langle n_d \rangle$. On the other hand, both GA and HFA give the correct³⁰ gap behavior for larger values of D .

In Fig. 4 we present the energy differences $\Delta E/V$ between the NM and F states, and the AF ground state, respectively. The F states are stable with respect to the NM ones only for sufficiently large D/V , where we show the respective results. Looking at the result of HFA, one notices that the energy difference between the NM and AF states increase rather fast with the value of D/V . For large U/D , the F state is stable against the NM one al-

ready for substantially lower values of D/V than in the case of small U/D . In general, the $\text{NM} \rightarrow F$ instability takes place at a similar value of $\Delta E/V$ between the NM and AF state. The differences between the GA and HFA results in Fig. 4 can be seen to be largely due to a relative stabilization of the NM state, compared to the magnetic states, in the GA case. This behavior is of course expected since the energy of the NM states is significantly improved by using the GA. On the other hand, much less correlation energy may be gained in the symmetry-broken states with either F or AF LRO,⁵¹ and, consequently, the energy differences between the F and AF states do not change significantly.

This general feature is reproduced in more detail in Fig. 5, where we show the gain in ground-state energy of the AF and NM states in GA, relative to HFA (E_{corr}). We observe that this correlation energy increases rapidly for increasing D in the NM state. On the other hand, the correlation energy in the AF state goes to a maximum at a small moment and decreases for increasing D . This, of course, reflects the proper behavior of HFA in the localized limit, which we discussed before.

The result for the magnetic moment m and hole density $\langle n_d \rangle$ is presented in Fig. 6, using a ratio of $U/V=5$ representative for the HTSO. We first observe that the d -hole density is substantially larger in GA than in HFA in the NM state. The increase of $\langle n_d \rangle$ by correlation effects was found before using the method of *local an-*

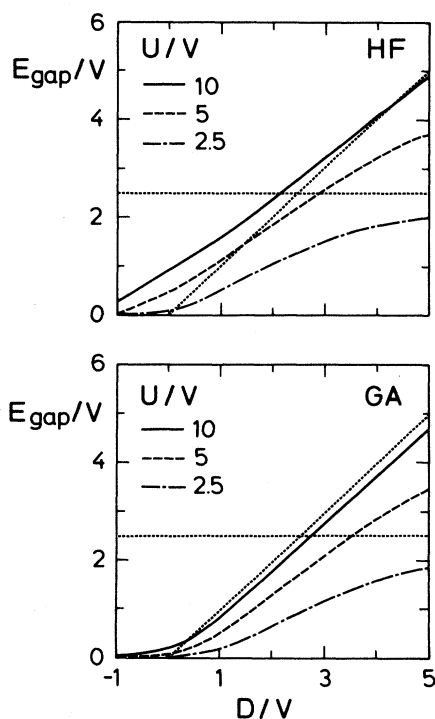


FIG. 3. Antiferromagnetic gap E_{gap}/V for $U/V=2.5, 5,$ and 10 , found in the HFA (upper part) and by using the GA (lower part), as a function of charge transfer energy D/V for the filling of one hole per unit cell of the CuO_2 plane ($N=1$).

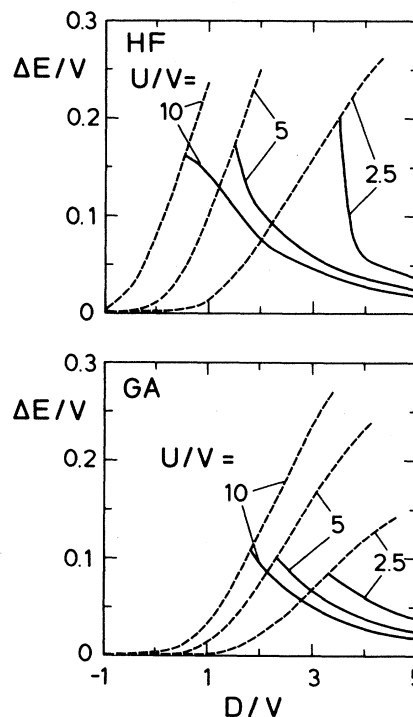


FIG. 4. Energy gain due to the AF order $\Delta E/V$ with respect to the nonmagnetic (dashed lines) and ferromagnetic (solid lines) state for $U/V=2.5, 5,$ and 10 , found in the HFA (upper part) and by using the GA (lower part), as a function of charge transfer energy D/V for $N=1$.

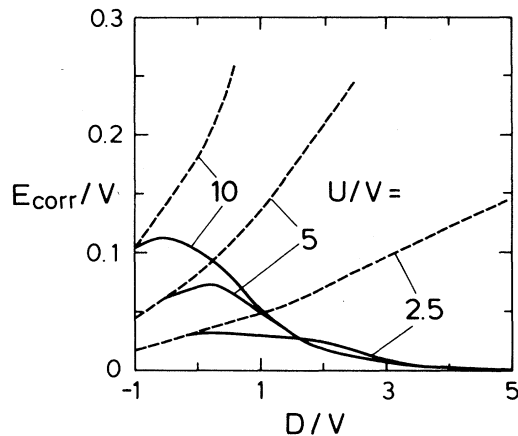


FIG. 5. Gain in the correlation energy E_{corr}/V defined as the difference between the energies found in HFA and GA in the AF (solid lines) and NM (dashed lines) states, as a function of charge transfer energy D/V for $U/V=2.5, 5$, and 10 , and for $N=1$.

*satz*¹⁹ for a model of the CuO_2 planes.²⁰ The actual number for the density change in GA ≈ 0.1 is in fact in good agreement with the latter more realistic model calculation. Turning to the AF state, it is seen that HFA predicts now *more* d holes than GA. According to the HFA, mo-

ment formation would give rise to a strong redistribution of charge. This is to some extent an artifact and it is seen that in GA this moment-charge coupling is much smaller. We finally observe that the moment starts to develop later in GA than in HFA for increasing D , as expected from our discussion in Sec. III.

So far, we have shown the dependence of several properties of the ground state as a function of the parameters appearing in the model Hamiltonian Eq. (2.1). However, we argued in Sec. III that in the localized limit both the HFA and the GA reduce to the same picture, while at low hole density we showed that the GA can be mapped onto a highly *renormalized* HFA (Stoner) theory. The question then arises to what extent this mapping is possible in the intermediate-coupling regime. For convenience, we only considered the simplest case where we renormalize D , to account for the different hole counts in HFA and GA. From the discussion in Sec. III it is clear that this will lead to errors for small $\langle n_d \rangle$ because in this limit U is strongly renormalized. Thus, we get an impression of how far the proper behavior of HFA in the localized regime extends into the intermediate-coupling regime if we compare GA and HFA results derived with the same U . Such a comparison is made in Fig. 7, where we compare E_{gap} vs m and m vs $\langle n_d \rangle$ as derived from GA and HFA, using $U/V=5$. We find a good agreement between HFA and GA as far as the gap dependence on m is concerned. On

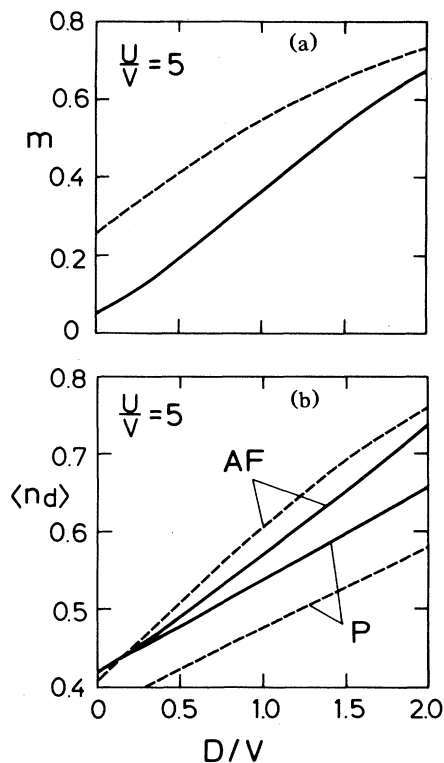


FIG. 6. (a) Hole density $\langle n_d \rangle$ in antiferromagnetic (AF) and paramagnetic states, and (b) magnetic moment m per Cu atom as functions of D/V for $U/V=5$ and $N=1$. Dashed and solid lines stand for HE and GA, respectively.

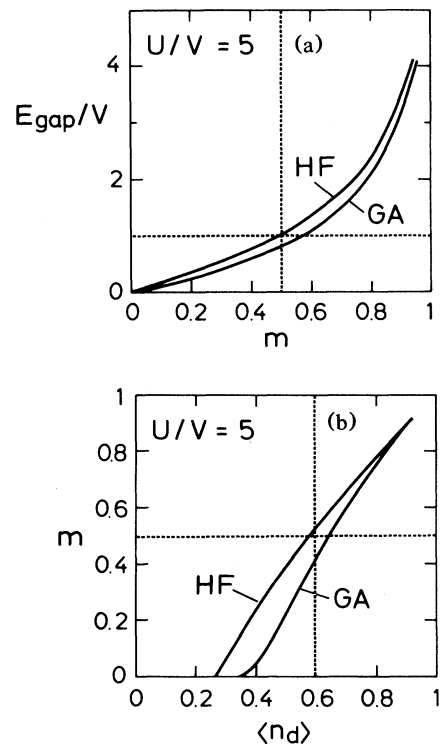


FIG. 7. (a) Magnetic moment m is a function of hole density $\langle n_d \rangle$, and (b) AF gap Δ/V as a function of magnetic moment m in HF (dashed lines) and GA (solid lines) for $U/V=5$, $V=1.8$ eV, and $N=1$. Dotted lines indicate the values of n_d and Δ/V for $0.4 < m < 0.6$.

the other hand, we notice significant differences in the dependence of m on $\langle n_d \rangle$, especially at low hole count. However, these deviations are by far not as pronounced as could be expected by looking at the low hole density limit, and thus we conclude that HFA is a quite good approximation to GA as long as the moment is sizable.

V. DISCUSSION AND CONCLUSIONS

In this paper we have presented a detailed analysis of the ground state of the two-band model at half filling, using GA and HFA. One finds that the instability of the band structure with respect to the formation of AF LRO is not removed by the correlation effects included in the GA, similarly as in the single-band Hubbard model.^{52,53} The overall picture we obtained may be summarized as follows: In the localized limit, HFA and GA converge to the same picture for the electronic structure, yielding a correct description of the AF ground state, except for the neglect of the quantum spin fluctuations. At low hole count $\langle n_d \rangle$ and large U , HFA is strongly in error and we have shown that GA behaves, at least in a qualitative way, more correctly. Further, we have derived a renormalized Stoner theory for this limit. Finally, we have studied numerically the intermediate-coupling regime, pointing out some significant differences between HFA and GA. Nevertheless, HFA is still a relatively good approximation if the system has a sizable moment, reflecting that the localized limit, in this restricted sense, is reached relatively quickly.

It is of interest to compare our result which follows from the effective Hamiltonian (3.14) for the NM phase at $U \rightarrow \infty$ with that of the slave-boson approach in the mean-field approximation.⁵⁴ We argue below that the system is metallic in the latter approximation for any value of D , with the Fermi level E_F crossing the bonding hole state narrowed by correlations close to its middle. Therefore, the interpretation of Kotliar, Lee, and Read⁵⁴ that from slave bosons a local charge-transfer gap that follows is spurious. This follows the equations which determine the average filling of the d level,

$$x = \frac{1}{2} \sum_{\mathbf{k}} (1 - \tilde{\xi}_{\mathbf{k}}^2) f(\tilde{\epsilon}_{\mathbf{k}}^-), \quad (5.1)$$

$$D - \tilde{D} = \left(\frac{2}{x} \right)^{1/2} V \sum_{\mathbf{k}} \tilde{\xi}_{\mathbf{k}} \tilde{\zeta}_{\mathbf{k}} \gamma_{\mathbf{k}} f(\tilde{\epsilon}_{\mathbf{k}}^-), \quad (5.2)$$

which have to be solved for the average number of slave bosons per Cu site, $x = 1 - \langle n_d \rangle$, and the renormalized charge transfer energy, $\tilde{D} = \epsilon_p - \tilde{\epsilon}_d$. The quasiparticle energies in the bonding hole band are

$$\tilde{\epsilon}_{\mathbf{k}}^- = \frac{1}{2} (\epsilon_p + \tilde{\epsilon}_d) = \frac{1}{2} [(\epsilon_p - \tilde{\epsilon}_d)^2 + 8\gamma_{\mathbf{k}}^2 x V^2]^{1/2}. \quad (5.3)$$

Therefore, by making this approximation one obtains, at $U \rightarrow \infty$, a different renormalization of the hybridization element than that given in Eq. (3.13) by a factor of $(1 - \frac{1}{2} \langle n_d \rangle)^{-1/2}$. As a consequence, the same structure of Eqs. (5.1) and (5.2) follows also from our effective Hamiltonian (3.14). Therefore, for the NM problem the *slave-boson* approach in the mean-field approximation is

equivalent to the GA provided that the value of V is changed by a factor of $\approx 2^{1/2}$. For a 1D Cu-O chain filled with $N=1$ hole per unit cell considered in Sec. IV, Eqs. (5.1) and (5.2) may be rewritten as follows:

$$x = \frac{1}{\pi} \int_0^{\pi/2} dz \left[1 - \frac{\tilde{D}}{(\tilde{D}^2 + 8xV^2 \sin^2 z)^{1/2}} \right], \quad (5.4)$$

$$\frac{D - \tilde{D}}{(32x)^{1/2}} = \frac{1}{\pi} \int_0^{\pi/2} dz \frac{V^3 \sin^3 z}{\tilde{D}^2 + 8xV^2 \sin^2 z}. \quad (5.5)$$

By solving them numerically one finds that a solution with $x > 0$ exists for any finite value of the only parameter D and that it gives a lower total energy than the insulating state (with $x=0$). Therefore, in the present two-band model no metal-insulator transition is found with increasing D , contrary to the Hubbard Hamiltonian.⁵⁵ This is consistent with the numerical results of Sec. IV following from the GA which is physically equivalent to the slave-boson picture for NM states.

Turning to the real materials (to HTSO, but also to the magnetic insulators in general), a first issue we want to address is the failure of the local spin-density approximation to describe the magnetism in these materials. The problem is that LSDA underestimates the spin polarization by roughly 1 order of magnitude.²¹ The kind of magnetism as realized in the HTSO is relatively rare. Although it is directly related to the antiferromagnetism of the usual magnetic insulators like the $3d$ oxides, the HTSO [as well as CuO (Ref. 56)] are exceptional because they are characterized by intermediate coupling. In fact, for the localized magnetic insulators the LSDA picture is internally inconsistent. On the one hand, there are several instances where it has been shown that LSDA results can be mapped onto Hubbard models, as we discussed in the Introduction. Especially, in cases characterized by large spin (e.g., MnO, or even NiO), the simple HFA treatment as discussed in this paper should be adequate. As a consequence, the two-particle interaction responsible for the magnetism should be the U as appearing in Eq. (2.1). In LSDA, however, things work out differently.⁵⁷ In the homogeneous electron gas, the spin-dependent part of the exchange-correlation potential is not directly related to the spin-independent part. As a consequence, it has been shown that, if the wave functions are sufficiently localized, an effective Stoner theory can be derived from the full LSDA.⁵⁸ For the case under consideration, this Stoner model is also roughly equivalent to our HFA model. The magnitudes of these LSDA Stoner parameters depend primarily on the charge density in the core regions of the ions and they are, therefore, characteristics of the ions. In the case of the truly itinerant magnets (e.g., elemental $3d$ metals), this approach is surprisingly successful, as shown by comparison between the results obtained from theories accounting for correlations in a more explicit way⁵¹ with experiment.⁵⁹ However, these LSDA Stoner parameters are typically an order of magnitude smaller than the on-site U 's to be used in the localized limit as Stoner parameters (see also Ref. 31). This order of magnitude error of LSDA has no significant consequences for the ground state of the strongly localized systems, because the bandwidths are even smaller than the LSDA Stoner splittings.

Consequently, an adequate description of the ground state of cases like NiO, etc. is found from LSDA.⁶⁰ However, the problem will become serious in systems with broader bands.

Also in our model treatment, an important renormalization of the U due to correlation is found in partially delocalized systems. However, the result is qualitatively different [Eq. (3.44)] from the ion-specific renormalizations of the LSDA. This suggests that the renormalizations in the case we studied are essentially different from those in conventional itinerant magnets, which is probably due to the existence of a gap. Moreover, in the case where one deals with a sizable moment (as in the HTSO), the renormalization of the U is relatively unimportant, as we have shown in Sec. IV. Therefore, it is expected that if one could construct a LSDA theory, in which the Stoner parameter is derived directly from the Hartree- and spin-independent exchange-correlation potentials, a much better description of the magnetism could be derived in intermediate-coupling cases like the HTSO.

Finally, let us turn to the HTSO magnetism in detail. We find a surprisingly good agreement between the overall picture for the electronic structure, as suggested by high-energy spectroscopies, and the ground-state magnetic properties. This can be deduced from Fig. 7. We note that, on the desired level of accuracy, the differences between the 1D and 2D lattices are rather insignificant if the moment is well developed, as we checked for HFA. The reason is that according to our findings in the preceding paragraph, the system is already quite localized, and in the localized limit dimensionality is unimportant for classical spins at zero temperature. Taking $U/V=5$ for the HTSO, as suggested by LSDA and experiment, and $\langle n_d \rangle \approx 0.6$ as found from the interpretation of core-XPS,²²⁻²⁵ we find $m \approx 0.5$, in agreement with the neutron data.⁵⁻⁷ Moreover, for such a moment (or d hole count), it follows that $E_{\text{gap}} \approx V$. Thus, taking $V \approx 1.5$ eV, our mean-field picture predicts a gap of the order of 2 eV, as observed experimentally.^{61,62} Finally, by looking at Fig. 4 we observe that a superexchange constant J is expected to be of the order of $0.1V$, i.e., $J \approx 1600$ K. A similarly large J has indeed been found by analyzing neutron data, where an in-plane exchange integral $J_{\parallel} = 1300$ K was reported.⁶³ This unusually large J implies that a large covalent reduction of the moment has to take place.²³

Up to this point, we have only considered the filling of $N=1$ hole per unit cell in the CuO_2 plane. However, a sensible theory should also account for the fast collapse of the AF LRO under doping. At first sight, it seems that one encounters here the difficulty of mean-field approaches because the moment disappears too slowly. In Fig. 8 we present the dependence of the magnetic moment m on the number of additional holes $\delta=N-1$ in the CuO_2 plane, in HFA and GA, using parameters representative for the HTSO. By taking into account the correlation effects by means of the GA, one reduces the critical doping δ_c for the disappearance of AF order from 0.24 to 0.13, if the moment is $0.4\mu_B$ at $\delta=0$, as assumed in Fig. 8; for a larger value of $m(\delta=0)$, AF LRO exists up to a higher value of δ_c . We notice that the decreasing magnet-

ic moment is accompanied by rather small changes of d -hole density $\langle n_d \rangle$ with increasing δ , so the excess holes are dominantly of oxygen character, as observed experimentally.⁶⁴ However, the results in Fig. 8 are obtained *assuming a uniform order parameter*. This is not correct; recently it has been shown that the true mean-field ground state in the doped systems contains discommensurations in this parameter regime⁶⁵ ("charged magnetic domain lines") which destroy the long-range spin order at arbitrarily low doping, while at the same time most of the moments are unchanged, in agreement with the neutron data.¹³ These discommensurations are intrinsically related to the nonlocal nature of the gap.

One could be satisfied with the picture for the HTSO as presented above. However, there is one big problem: *the moment as observed in the HTSO is too large*. In our mean-field treatment we have neglected the quantum spin fluctuations (QSF). On the other hand, it is known that the QSF are extremely important in the localized limit. For instance, in the 2D, $S = \frac{1}{2}$ Heisenberg model, the magnetic moment is reduced down to $0.36\mu_B - 0.38\mu_B$.^{14,15} Adding this reduction to that coming from the charge fluctuations as discussed in this paper, one would expect a much smaller moment than measured experimentally. Indeed, preliminary Monte Carlo results⁶⁶ indicate a vanishing moment in the parameter regime we have focused on. Apparently, the two-band model is not able to describe the electronic structure and the magnetic properties

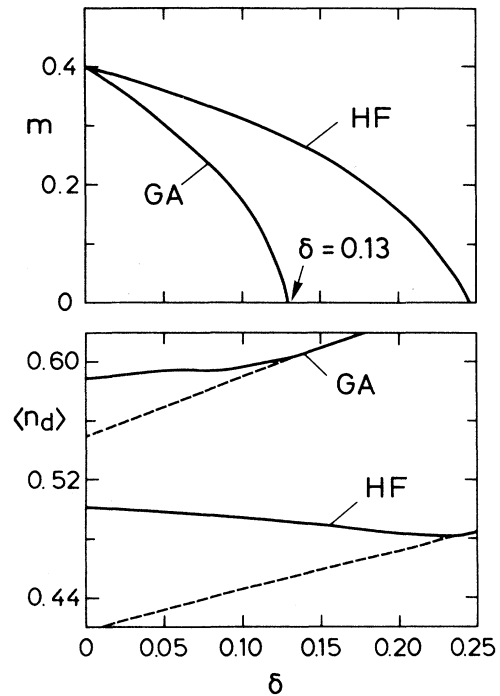


FIG. 8. (a) Magnetic moment m and (b) hole density $\langle n_d \rangle$ in the AF ground state (solid lines) and in the corresponding NM state (dashed lines), as functions of doping $\delta=N-1$ in the HFA and by using GA for $U/V=5$. The value of charge transfer energy $D/V=0.45$ and ≈ 1.1 for HF and GA, respectively, was chosen to give the magnetic moment $m = 0.4$ at $\delta=0$.

of the HTSO at the same time. Thus, the model is incomplete.

Although it cannot be excluded that something fundamental is missing from our understanding of the global electronic structure, we tend to think that a more likely candidate for revision is the (localized) picture of the magnetism in the HTSO. First, the interpretation of the electronic structure relates to straightforward quantities like the magnitude of the band gap, $\langle n_d \rangle$, transfer integrals, etc. For instance, it is hard to believe that a p - d transfer integral V can be much different from 1 eV in a $3d$ system [see, among numerous other examples, the success of LDA for Cu_2O (Ref. 67)]. Trying to cure the moment problem by revising this picture would result in an extremely unlikely outcome; according to quantum Monte Carlo calculations $D/V \geq 6$.⁶⁶

On the other hand, the interpretation of the spin-only properties is a much more subtle affair, involving issues like the effective dimensionality, the exact (quantum or classical?) nature of the spin Hamiltonian, whether charge degrees of freedom are important, etc. In fact, there are a couple of experimental indications that the "standard"^{7,13} understanding of the HTSO magnetism is misleading. According to the analysis of Tranquada *et al.*⁷ and Birgeneau *et al.*,¹³ the magnetism in La_2CuO_4 is extremely 2D. According to this work, one contribution comes from the magnetic frustration between the planes. However, the renormalization of the moment due to QSF is expected not to be influenced by this frustration effect and this is not considered in the analysis of Ref. 68. Also, these authors end up with an extremely small effective J_\perp of several mK,⁶⁹ being by about 5 orders of magnitude smaller than J_\parallel . The former exchange integral is expected to be of the same order of magnitude in $\text{YBa}_2\text{Cu}_3\text{O}_6$ as in La_2CuO_4 , at least as we consider the magnitude of the moment. How can we explain then the much larger moment in $\text{YBa}_2\text{Cu}_3\text{O}_6$? The local environment of Cu and O in CuO is similar to that in the HTSO and one expects a similar covalency, in agreement with spectroscopic findings.⁶⁷ However, CuO is magnetically 3D and, nevertheless, the same moment [$\approx 0.68\mu_B$ (Ref. 70)] is found as in $\text{YBa}_2\text{Cu}_3\text{O}_6$ [$\approx 0.66\mu_B$ (Ref. 7)]. Also striking is the observation by Aeppli and Buttrey⁷¹ that the 2D magnetic fluctuations in La_2NiO_4 are very similar to those in La_2CuO_4 , although the former system has $S \approx 1$. We also note that the fluctuations in this system disappear in the (fully frustrated) tetragonal phase, indicating that the third dimension plays some critical role in the slowing down of the 2D fluctuations. In addition, it has been argued that, contrary to the claims of Tranquada *et al.*⁶ and Birgeneau *et al.*,¹³ the neutron line shapes as observed in La_2CuO_4 cannot be explained in the 2D Heisenberg framework.⁷² Finally, the most striking difficulty is the recent observation by Lynn *et al.*⁷³ of a low-temperature AF phase in $\text{YBa}_2\text{Cu}_3\text{O}_6$, shown in moments of $\approx 0.97\mu_B$ in the planes and $\approx 0.4\mu_B$ in the chains. We agree with the conjecture of these authors that this indicates a more 3D and itinerant magnetism than is assumed in the standard picture. In this respect, it would be interesting to sort out what theory has to tell about the magnetic dimensionality (for instance, the $\text{La } 3d\text{-O } 2p$

transfer integral is surprisingly large ≈ 1 eV) and to see if in this way the models for the HTSO can be improved.

ACKNOWLEDGMENTS

We would like to thank P. Fazekas, O. Gunnarsson, P. Horsch, G. A. Sawatzky, and G. Stollhoff for valuable discussions, as well as O. K. Andersen and P. Fulde for their stimulating support and valuable remarks. One of us (A.M.O.) acknowledges the financial support of the Polish Research Project No. CPBP 01.09.

APPENDIX: GUTZWILLER ANSATZ FOR A FINITE CLUSTER

We show below that the exact ground-state energy of the cluster which consists of one Cu atom surrounded by four O atoms and filled with two holes within Cu $3d$ and O $2p$ orbitals is rigorously reproduced by the Gutzwiller method adopted in Sec. III. The cluster is charged and may be formally written as CuO_4^{5-} . We assume that the holes within the cluster are described by the model Hamiltonian (2.1) and take $\epsilon_p = 0$. It is convenient to choose the basis states of p holes as four combinations of the atomic states $|m\rangle = a_{m\sigma}^\dagger |0\rangle$, with a σ hole localized on the m th oxygen site, which correspond to the irreducible representations of the symmetry group D_{4h} of the considered square. Only the symmetric combination,

$$|p\sigma\rangle = a_{p\sigma}^\dagger |0\rangle = \frac{1}{2} (|1\rangle + |2\rangle + |3\rangle + |4\rangle), \quad (\text{A1})$$

couples to the $|d\sigma\rangle$ state at the Cu site. Having two holes of opposite spins in the system, the exact ground state is found by diagonalizing the matrix

$$M_0 = \begin{pmatrix} 2\epsilon_d + U & 2^{1/2}V & 0 \\ 2^{1/2}V & \epsilon_d & 2^{1/2}V \\ 0 & 2^{1/2}V & 0 \end{pmatrix}. \quad (\text{A2})$$

Let us consider for simplicity the $U \rightarrow \infty$ limit of Eq. (A2), in which the ground-state energy $\epsilon_0^{\text{ex}} = E_0/V$ is

$$\epsilon_0^{\text{ex}} = \frac{1}{2}p - \frac{1}{2}(p^2 + 8)^{1/2}, \quad (\text{A3})$$

where we have used $p = \epsilon_d/V$. The number of d holes in the ground state is given by

$$\langle n_d \rangle = \frac{1}{2} - \frac{p}{2(p^2 + 8)^{1/2}}. \quad (\text{A4})$$

In the GA one instead diagonalizes the matrix

$$M_{\text{GA}} = \begin{pmatrix} \bar{\epsilon}_d & q^{1/2}V \\ q^{1/2}V & 0 \end{pmatrix}, \quad (\text{A5})$$

where q is the renormalization factor (3.14) derived in Sec. III,

$$q = \frac{1 - \langle n_d \rangle}{1 - \frac{1}{2}\langle n_d \rangle}. \quad (\text{A6})$$

The ground-state energy has to be found now by minimiz-

ing the expression

$$\varepsilon_0^{\text{GA}} = 2\omega_- + \mu \langle n_d \rangle, \quad (\text{A7})$$

where ω_- is the lower eigenvalue of M_{GA} ,

$$\omega_- = \frac{1}{2} \bar{p} - \frac{1}{2} (\bar{p} + 4q)^{1/2}, \quad (\text{A8})$$

and $\bar{p} = (\varepsilon_d/V - \mu)$. The chemical potential μ is measured in the units of V and has to be found from the minimization procedure.

For the particular form of the energy (A7), it is convenient to express the chemical potential μ as a function of average hole density $\langle n_d \rangle$, defined in the case of GA by

$$\langle n_d \rangle = 1 - \frac{\bar{p}}{(\bar{p}^2 + 4q)^{1/2}}. \quad (\text{A9})$$

By introducing

$$x = 1 - \langle n_d \rangle, \quad (\text{A10})$$

and using the expression for the renormalization factor q , we find that

$$\bar{p}^2 = \frac{8x^3}{(x+1)^2(1-x)}. \quad (\text{A11})$$

The final form of energy,

$$\varepsilon_0^{\text{GA}} = p(1-x) - 2[2x(1-x)]^{1/2}, \quad (\text{A12})$$

is now obtained by inserting Eqs. (A8) and (A11) into (A7) and by using the definition of chemical potential μ . The energy $\varepsilon_0^{\text{GA}}$ may now be easily minimized with respect

to the variable x . The condition for the minimum gives

$$x = \frac{1}{2} + \frac{p}{2(p^2+8)^{1/2}}. \quad (\text{A13})$$

In this way we recover Eq. (A4). It is now straightforward to see that the exact ground-state energy $\varepsilon_0^{\text{ex}}$ is reproduced when the solution (A13) is inserted into Eq. (A12).

We notice that, in spite of reproducing the ground-state energy by combining the two lower eigenvalues of \uparrow - and \downarrow -hole subspaces of the effective Hamiltonian (3.14) with the product of $\mu \langle n_d \rangle$, we do not find any correspondence between the excited states which follow from the GA and the rigorous ones. The quasiparticle states introduced as eigenstates of the effective Hamiltonian have to be considered only as effective energies for the system filled by a given number of holes, similarly for the energies of HF states.

In closing, we would like to point out that the present problem is formally equivalent to a two-orbital model considered in heavy-fermion physics,⁷⁴ so in this case also the GA reproduces the exact ground-state energy and the charge distribution. In this model, one of the orbitals is strongly correlated, having large Coulomb interaction U , whereas the other stands for an uncorrelated conduction electron band. In fact, the two-orbital model may be derived from the Wolff model for a magnetic impurity in a nonmagnetic matrix by means of the GA (Ref. 49), and therefore it gives the simplest physical insight into the nature of low-energy singlet-triplet excitation.⁷⁴

*Permanent address: Institute of Physics, Jagellonian University, PL-30059 Kraków, Poland.

¹P. Fulde, *Physica C* **153-155**, 1769 (1988).

²C. M. Varma (unpublished).

³M. Cyrot, *J. Phys. (Paris)* (to be published).

⁴Y. Kitaoka, K. Ishida, T. Kobayashi, K. Amaya, and K. Asayama, *Physica C* **153-155**, 733 (1988).

⁵D. Vaknin, S. K. Sinha, D. E. Moneton, D. C. Johnston, J. M. Newsam, C. R. Safinya, and H. E. King, Jr., *Phys. Rev. Lett.* **58**, 2802 (1987).

⁶J. M. Tranquada, D. E. Cox, W. Kunmann, H. Moudden, G. Shirane, P. Zolliker, D. Vaknin, S. K. Sinha, M. S. Alvarez, A. J. Jacobson, and D. C. Johnston, *Phys. Rev. Lett.* **60**, 156 (1988); W. H. Li, J. W. Lynn, H. A. Mook, B. S. Sales, and Z. Fisk, *Phys. Rev. B* **37**, 9844 (1988).

⁷J. M. Tranquada, A. H. Moudden, A. I. Goldman, P. Zolliker, D. E. Cox, G. Shirane, S. K. Sinha, D. Vaknin, D. C. Johnston, M. S. Alvarez, and A. J. Jacobson, *Phys. Rev. B* **38**, 2477 (1988).

⁸Y. J. Uemura, *J. Phys. (Paris)* (to be published).

⁹P. W. Anderson, *Science* **235**, 1196 (1987); P. W. Anderson, G. Baskaran, Z. Zou, and T. Hsu, *Phys. Rev. Lett.* **58**, 2790 (1987); M. Cyrot, *Solid State Commun.* **62**, 821 (1987); A. E. Ruckenstein, P. J. Hirschfeld, and J. Appel, *Phys. Rev. B* **36**, 857 (1987).

¹⁰J. R. Schrieffer, X. G. Wen, and S. C. Zhang, *Phys. Rev. Lett.* **60**, 944 (1988).

¹¹V. J. Emery, *Phys. Rev. Lett.* **58**, 2794 (1987); J. E. Hirsch, *ibid.* **59**, 229 (1987).

¹²D. R. Harshman, G. Aeppli, G. P. Espinosa, A. S. Cooper, J.

P. Remeika, E. J. Ansaldo, T. M. Riseman, D. L. Williams, D. R. Noakes, B. Ellman, and T. F. Rosenbaum, *Phys. Rev. B* **38**, 852 (1988).

¹³J. Birgeneau, D. R. Gabbe, H. P. Jenness, M. A. Kastner, P. J. Picone, T. R. Thurston, G. Shirane, Y. Endoh, M. Sato, K. Yamada, Y. Hidaka, M. Oda, Y. Enomoto, M. Suzuki, and T. Marakami, *Phys. Rev. B* **38**, 6614 (1988).

¹⁴S. Chakravarty, B. I. Halperin, and D. R. Nelson, *Phys. Rev. Lett.* **60**, 1057 (1988).

¹⁵P. Horsch and W. von der Linden, *Physica C* **153-155**, 1285 (1988).

¹⁶A. Aharony, R. J. Birgeneau, A. Coniglio, M. A. Kastner, and H. E. Stanley, *Phys. Rev. Lett.* **60**, 1330 (1988).

¹⁷L. F. Mattheiss, *Phys. Rev. Lett.* **58**, 1028 (1987).

¹⁸K. C. Hass, *Solid State Physics*, edited by H. Ehrenreich and D. Turnbull (Academic, Orlando, 1989), Vol. 42.

¹⁹A. M. Oleś, J. Zaanen, and P. Fulde, *Physica B* **148**, 260 (1987).

²⁰A. M. Oleś and J. Zaanen, *Int. J. Mod. Phys. B* **1**, 751 (1988).

²¹J. Zaanen, O. Jepsen, O. Gunnarsson, A. T. Paxton, O. K. Andersen, and A. Svane, *Physica C* **153-155**, 1636 (1988).

²²A. Fujimori, E. Takayama-Muromachi, Y. Uchida, and B. Okai, *Phys. Rev. B* **35**, 8814 (1987).

²³Z. Shen, J. W. Allen, J. J. Yeh, J. S. Kang, W. Ellis, W. Spicer, I. Lindau, M. P. Maple, Y. D. Dalichaouch, M. S. Torikachvili, J. Z. Sun, and T. H. Geballe, *Phys. Rev. B* **36**, 8414 (1987).

²⁴J. C. Fuggle, P. J. W. Weiss, R. Schoorl, G. A. Sawatzky, J. Fink, N. Nücker, P. J. Durham, and W. M. Temmerman, *Phys. Rev. B* **37**, 123 (1988).

- ²⁵H. Eskes and G. A. Sawatzky, *Phys. Rev. Lett.* **61**, 1415 (1988).
- ²⁶N. G. Stoffel, Y. Chang, M. K. Kelly, L. Döttl, M. Onellion, P. A. Morris, W. A. Bonner, and G. Margaritondo, *Phys. Rev. B* **37**, 7952 (1988).
- ²⁷T. Takahashi, H. Matsuyama, H. Katayama-Yoshida, Y. Okabe, S. Hosoya, K. Seki, H. Fujimoto, M. Sato, and H. Inokuchi, *Nature (London)* **334**, 691 (1988).
- ²⁸Y. Petroff, in *Proceedings of the IBM Europe Institute Workshop on High- T_c Superconductivity*, Oberlech, 1988 (unpublished).
- ²⁹C. M. Varma, S. Schmitt-Rink, and E. Abrahams, *Solid State Commun.* **62**, 681 (1987).
- ³⁰J. Zaanen, G. A. Sawatzky, and J. W. Allen, *Phys. Rev. Lett.* **55**, 418 (1985).
- ³¹J. Zaanen and G. A. Sawatzky, *Can. J. Phys.* **65**, 1262 (1987).
- ³²J. Zaanen and A. M. Oleś, *Phys. Rev. B* **37**, 9423 (1988).
- ³³P. W. Anderson, *Phys. Rev.* **115**, 2 (1959).
- ³⁴D. E. Eastman, F. J. Himpsel, and J. A. Knapp, *Phys. Rev. Lett.* **40**, 1514 (1978); F. J. Himpsel, J. A. Knapp, and D. E. Eastman, *Phys. Rev. B* **19**, 2919 (1979); W. Eberhardt and E. W. Plummer, *ibid.* **21**, 3245 (1980).
- ³⁵O. Gunnarsson, *J. Phys. F* **6**, 587 (1976); A. M. Oleś and G. Stollhoff, *J. Magn. Magn. Mat.* **54-57**, 1045 (1986).
- ³⁶S. Massida, J. Yu, A. J. Freeman, and D. D. Koelling, *Phys. Lett. A* **122**, 198 (1987); J. Yu, S. Massida, A. J. Freeman, and D. D. Koelling, *ibid.* **122**, 203 (1987).
- ³⁷M. S. Hybertsen and L. F. Mattheiss, *Phys. Rev. Lett.* **60**, 1661 (1988); L. F. Mattheiss and D. R. Hamann, *Phys. Rev. B* **38**, 5012 (1988).
- ³⁸D. R. Hamann and L. F. Mattheiss, *Phys. Rev. B* **38**, 5138 (1988).
- ³⁹M. Schluter, J. Hybertsen, and N. E. Christensen, *Physica C* **153-155**, 1217 (1988).
- ⁴⁰E. B. Stechel and D. R. Jennison, *Phys. Rev. B* **38**, 4632 (1988).
- ⁴¹J. Barnasconi, *Phys. Kondens. Mater.* **14**, 225 (1972).
- ⁴²M. C. Gutzwiller, *Phys. Rev.* **137**, A1726 (1965).
- ⁴³T. M. Rice and K. Ueda, *Phys. Rev. B* **34**, 6420 (1986).
- ⁴⁴C. M. Varma, W. Weber, and L. J. Randall, *Phys. Rev. B* **33**, 1015 (1985).
- ⁴⁵P. Fazekas and B. H. Brandow, *Phys. Scr.* **36**, 809 (1987).
- ⁴⁶V. Z. Vulović and E. Abrahams, *Phys. Rev. B* **36**, 2614 (1987).
- ⁴⁷H. Yokoyama and H. Shiba, *J. Phys. Soc. Jpn.* **56**, 3570 (1987).
- ⁴⁸D. Vollhardt, *Rev. Mod. Phys.* **56**, 99 (1984).
- ⁴⁹K. A. Chao, A. M. Oleś, and J. Spałek, *Phys. Rev. B* **17**, 4339 (1978); K. A. Chao and A. M. Oleś, *Physica B* **106**, 320 (1981).
- ⁵⁰P. Fazekas, *Solid State Commun.* **60**, 431 (1986).
- ⁵¹See, e.g., P. Fulde, Y. Kakehashi, and G. Stollhoff, in *Metallic Magnetism*, edited by H. Capellmann, *Topics in Current Physics*, Vol. 42 (Springer-Verlag, Berlin, 1987); A. M. Oleś, *J. Phys. (Paris)* (to be published).
- ⁵²K. Kubo and M. Uchinami, *Prog. Theor. Phys.* **54**, 1259 (1975); A. M. Oleś and J. Spałek, *Z. Phys. B* **44**, 177 (1981).
- ⁵³W. Metzner and D. Vollhardt, *Phys. Rev. Lett.* **59**, 121 (1987).
- ⁵⁴G. Kotliar, P. A. Lee, and N. Read, *Physica C* **153-155**, 538 (1988).
- ⁵⁵W. F. Brinkman and T. M. Rice, *Phys. Rev. B* **2**, 4302 (1970).
- ⁵⁶O. Jepsen (private communication).
- ⁵⁷A. Svane and O. Gunnarsson, *Europhys. Lett.* **7**, 171 (1988).
- ⁵⁸O. Gunnarsson, *J. Phys. F* **6**, 587 (1976).
- ⁵⁹J. F. Cooke, J. W. Lynn, and H. L. Davis, *Phys. Rev. B* **21**, 4118 (1980).
- ⁶⁰K. Terakura, T. Oguchi, A. R. Williams, and J. Kübler, *Phys. Rev. B* **30**, 4934 (1984).
- ⁶¹J. M. Ginder, M. G. Roe, Y. Song, R. P. McCall, J. R. Gaines, E. Ehrenfreund, and A. J. Epstein, *Phys. Rev. B* **37**, 7506 (1988).
- ⁶²U. Venkateswaran, K. Strössner, M. Hanfland, M. Holtz, K. Syassen, and H. Mattausch (unpublished).
- ⁶³G. Shirane, Y. Endoh, R. J. Birgeneau, M. A. Kastner, Y. Hidaka, M. Oda, M. Suzuki, and T. Murakami, *Phys. Rev. Lett.* **59**, 1613 (1988).
- ⁶⁴N. Nücker, J. Fisk, J. C. Fuggle, P. J. Durham, and W. M. Temmerman, *Phys. Rev. B* **37**, 5158 (1988).
- ⁶⁵J. Zaanen and O. Gunnarsson (unpublished).
- ⁶⁶A. Muramatsu (private communication).
- ⁶⁷G. A. Sawatzky, *Int. J. Mod. Phys. B* **1**, 779 (1988).
- ⁶⁸C. J. Peters, R. J. Birgeneau, M. A. Kastner, Y. Yoshizawa, Y. Endoh, J. Tranquada, G. Shirane, Y. Hidaka, M. Oda, M. Suzuki, and T. Murakami, *Phys. Rev. B* **37**, 9761 (1988).
- ⁶⁹Y. Endoh, K. Yamada, R. J. Birgeneau, D. R. Gabbe, H. P. Janssen, M. A. Kastner, C. J. Peters, P. J. Picone, T. R. Thurston, J. M. Tranquada, G. Shirane, Y. Hidaka, M. Oda, Y. Enomoto, M. Suzuki, and T. Murakami, *Phys. Rev. B* **37**, 7443 (1988).
- ⁷⁰B. N. Brockhouse, *Phys. Rev.* **94**, A781 (1954); B. X. Yang, J. M. Tranquada, and G. Shirane, *Phys. Rev. B* **38**, 174 (1988).
- ⁷¹G. Aeppli and D. J. Buttrey, *Phys. Rev. Lett.* **61**, 203 (1988).
- ⁷²D. R. Grempel, *Phys. Rev. Lett.* **61**, 1041 (1988).
- ⁷³J. W. Lynn, W. H. Li, H. A. Mook, B. C. Sales, and Z. Fisk, *Phys. Rev. Lett.* **60**, 2781 (1988).
- ⁷⁴P. Fulde, *J. Phys. F* **18**, 601 (1988).